



# Forest-floor greenhouse gas fluxes in a subalpine spruce forest: Continuous multi-year measurements, drivers, and budgets

Luana Krebs<sup>1</sup>, Susanne Burri<sup>1</sup>, Iris Feigenwinter<sup>1</sup>, Mana Gharun<sup>2</sup>, Philip Meier<sup>1</sup>, Nina Buchmann<sup>1</sup>

<sup>1</sup>Department of Environmental Systems Science, Institute of Agricultural Sciences, ETH Zurich, Switzerland

5 <sup>2</sup>Faculty of Geosciences, Institute of Landscape Ecology, University of Munster, Germany

*Correspondence to:* Luana Krebs (luana.krebs@usys.ethz.ch)

**Abstract.** Forest ecosystems play an important role in the global carbon (C) budget by sequestering a large fraction of anthropogenic carbon dioxide (CO<sub>2</sub>) emissions and by acting as important methane (CH<sub>4</sub>) sinks. The forest-floor greenhouse gas (GHG; CO<sub>2</sub>, CH<sub>4</sub> and nitrous oxide N<sub>2</sub>O) flux, i.e., from soil and understory vegetation, is one of the major components to consider when determining the C budget of forests. Although winter fluxes are essential to determine the annual C budget, only very few studies have examined long-term, year-round forest-floor GHG fluxes. Thus, we aimed to i) quantify the seasonal and annual variations of forest-floor GHG fluxes; ii) evaluate their drivers, including the effects of snow cover, timing, and amount of snow melt, and iii) calculate annual budgets of forest-floor GHG fluxes for a subalpine spruce forest in Switzerland. We measured GHG fluxes year-round during four years with four automatic large chambers at the ICOS Class 1 Ecosystem station Davos (CH-Dav). We applied random forest models to investigate environmental drivers and to gap-fill the flux time series. Annual and seasonal forest-floor CO<sub>2</sub> emissions responded most strongly to soil temperature and snow depth (2.34±0.20 kg CO<sub>2</sub> m<sup>-2</sup> yr<sup>-1</sup>). No response of forest-floor CO<sub>2</sub> emissions to leaf area index or photosynthetic photon flux density was observed, suggesting a strong direct control of environmental factors and a weak or even lacking indirect control of canopy biology. Furthermore, the forest-floor was a consistent CH<sub>4</sub> sink (-19.1±1.8 g CO<sub>2</sub>-eq m<sup>-2</sup> yr<sup>-1</sup>), with annual fluxes driven mainly by snow depth. Fluxes during winter were less important for the CO<sub>2</sub> budget (6.0–7.3 %), while they contributed substantially to the annual CH<sub>4</sub> budget (14.4–18.4 %). N<sub>2</sub>O fluxes were very low, negligible for the forest-floor GHG budget at our site. In 2022, the warmest year on record with also below-average precipitation at the Davos site, we observed a substantial increase in forest-floor CO<sub>2</sub> emissions compared to other years. The mean forest-floor GHG budget indicated emissions of 2317±200 g CO<sub>2</sub>-eq m<sup>-2</sup> yr<sup>-1</sup> (mean±standard deviation over four years), with CO<sub>2</sub> fluxes dominating and CH<sub>4</sub> offsetting a small proportion (0.8 %) of the GHG budget. Due to the relevance of snow cover, we recommend year-round measurements of GHG fluxes with high temporal resolution. In a future with increasing temperatures and less snow cover due to climate change, we expect increased forest-floor CO<sub>2</sub> emissions even at this subalpine site, with negative effects on its carbon sink behaviour.



## 1 Introduction

30 Carbon dioxide (CO<sub>2</sub>), methane (CH<sub>4</sub>), and nitrous oxide (N<sub>2</sub>O) are the three main greenhouse gases (GHGs) driving global warming. Forest ecosystems play an important role in the global carbon (C) cycle by sequestering a large fraction of anthropogenic CO<sub>2</sub> emissions and by acting as an important CH<sub>4</sub> sink (Borken et al., 2006; Ni and Groffman, 2018). The GHG flux of the forest-floor, i.e., soil and understory vegetation, is one of the major components to consider when determining the C budget of forests, since soil respiration is the second largest terrestrial C flux and accounts for approximately 70 % of CO<sub>2</sub> losses in temperate forests (IPCC, 2021; Yuste et al., 2005). However, how forest-floor GHG fluxes will respond to climate change is still largely unknown.

Global warming particularly affects high latitude and high altitude forests (IPCC, 2021), altering snowfall, length and timing of snow cover as well as melting and soil freeze-thaw cycles (CH2018, 2018; Klein et al., 2016). Nevertheless, there have been very few studies that examined continuous, year-round and long-term forest-floor GHG fluxes in high latitude or high altitude forests (Barba et al., 2019; Luo et al., 2011). Unfortunately, measurements during periods with snow cover are challenging and thus often lacking due to logistical reasons, leading to winter fluxes missing even from multi-year studies (e.g., Richardson et al., 2019).

The forest-floor's CO<sub>2</sub> fluxes involve the processes of photosynthetic CO<sub>2</sub> uptake by plants as well as autotrophic and heterotrophic respiratory losses from plants and soils, respectively (Hanson et al., 2000). All three processes and their contributions to the total soil CO<sub>2</sub> fluxes depend on biotic and abiotic factors. For example, autotrophic respiration is mainly driven by plant activity and hence linked to photosynthesis and solar energy (Högberg et al., 2001; Janssens et al., 2001), whereas, heterotrophic respiration is strongly controlled by soil conditions (i.e., temperature and moisture), substrate availability, and the microbial community (e.g., Janssens et al., 2001; Scott-Denton et al., 2006). Furthermore, winter dynamics can impact soil respiration rates through changes in snow cover, soil freezing and thawing cycles (Reinmann and Templer, 2018; Schindlbacher et al., 2007). Especially, freeze-thaw events have recently been the focus of research because they cause abrupt changes in biophysical soil conditions which can alter autotrophic and heterotrophic soil respiration rates (Song et al., 2017). How the two components of soil respiration respond to climate change is however subject to major uncertainties with many studies showing contradictory results. Some studies demonstrated no significant increase of soil respiration to experimental warming in forest soils (Bradford et al., 2008; Carey et al., 2016), while others observed higher soil respiration rates (Bond-Lamberty et al., 2018; Crowther et al., 2016; Karhu et al., 2014). Among those reporting higher rates, there is disagreement on whether long-term adaptation can occur. In some studies, the higher respiration rates were sustained over several years (Melillo et al., 2017), while in others they declined again to previous levels (Eliasson et al., 2005; Hartley et al., 2007).

Forest soils have been shown to act as an atmospheric CH<sub>4</sub> sink (Dutaur and Verchot, 2007). The uptake of CH<sub>4</sub> in oxic soils occurs due to the presence of methanotrophic bacteria (Saunois et al., 2020). It is highly dependent on environmental factors, including soil temperature ( $T_{\text{soil}}$ ), soil texture (transport of CH<sub>4</sub> into the soil), soil moisture (transport of CH<sub>4</sub> into the soil and



limitation of bacterial activity), and soil nitrogen (N) content (Borken et al., 2006; Luo et al., 2013; Ni and Groffman, 2018). Furthermore, biotic factors such as plant cover can affect CH<sub>4</sub> consumption of the forest floor through the presence of *Sphagnum* moss species which are inhabited by methane-oxidizing bacteria (Basiliko et al., 2004). Generally, in temperate  
65 forests, CH<sub>4</sub> uptake increases in warmer and drier soils (Borken et al., 2006; Ni and Groffman, 2018). Winter dynamics further impact CH<sub>4</sub> fluxes, with frozen soil and snow cover affecting microbial activity and gas transport (Blankinship et al., 2018; Borken et al., 2006). Understanding the drivers of forest-floor CH<sub>4</sub> fluxes, including the complex interplay between biotic and abiotic factors, is vital for accurately modeling and predicting the role of forest ecosystems in the global CH<sub>4</sub> cycle.

Moreover, the forest-floor can act as a source or sink of N<sub>2</sub>O (Chapuis-Lardy et al., 2007; Goldberg et al., 2010). Soil  
70 temperature, soil moisture, and N availability significantly influence N<sub>2</sub>O fluxes through regulating the microbial processes which are mainly responsible for N<sub>2</sub>O production in soils, i.e., nitrification and denitrification (Schaufler et al., 2010). High N<sub>2</sub>O emission rates in temperate forests have been found under warm and moist conditions (Luo et al., 2013). Furthermore, studies have revealed that high N<sub>2</sub>O emissions occur during freezing-thawing cycles and rewetting events, when abrupt changes in temperature and moisture conditions promote microbial activity and thus the release of N<sub>2</sub>O (Goldberg et al., 2010; Papen  
75 and Butterbach-Bahl, 1999; Liu et al., 2018). Understanding the dynamics of these processes and drivers, particularly during freezing-thawing cycles, is crucial for estimating N<sub>2</sub>O emissions from forests.

In this study, we investigated combined measurements of CO<sub>2</sub>, CH<sub>4</sub> and N<sub>2</sub>O forest-floor fluxes in a subalpine Norway spruce forest (Davos, CH-Dav, ICOS Class 1 Ecosystem station), in response to biotic and environmental drivers, based on four years of continuous measurements (2017, 2020-2022). Our objectives were to i) quantify seasonal and annual variations in climate  
80 variables and forest-floor CO<sub>2</sub>, CH<sub>4</sub> and N<sub>2</sub>O fluxes; ii) evaluate the drivers of forest-floor GHG fluxes, including effects of snow cover, timing and amount of snow melt; and iii) calculate the annual budgets of forest floor GHG fluxes.

## 2 Methods

### 2.1 Study site

The study site is a subalpine evergreen coniferous forest, located in the eastern Swiss Alps at a mean altitude of 1640 m a.s.l.  
85 (Davos Seehornwald; CH-Dav; 46°48'55.2" N, 9°51'21.3" E). The total annual precipitation is 876 mm, and the mean annual temperature is 4.3 °C (1997–2022). The site is certified as ICOS (Integrated Carbon Observation System) Class 1 Ecosystem station for eddy-covariance flux measurements since 2019. The dominant species is Norway spruce (*Picea abies* (L.) Karst), with an average tree height of 18 m (max. 35 m), and a mean tree age of approx. 100 years (with some specimens reaching over 300 years). Understory vegetation covers about 30 % of the surface and is mainly composed of blueberry (*Vaccinium  
90 myrtillus* and *Vaccinium gaulterioides*) and mosses (*Sphagnum* sp. Ehrh.). CH-Dav is a sustainably managed forest according to the Swiss National Forest Protection Law (1876; Tschopp, 2012). The soil types are chromic cambisol and rustic podzol (FAO classification; Jörg, 2008; Tab. 1).



## 2.2 Chamber flux measurements

### 2.2.1 Chamber setup

95 Forest-floor CO<sub>2</sub>, CH<sub>4</sub> and N<sub>2</sub>O fluxes were measured during the years 2017 and 2020–2022 using a fully automated system with four chambers (FF1 to FF4) distributed within an area of 3600 m<sup>2</sup> in the forest, representative for the eddy-covariance footprint. Concentrations of CO<sub>2</sub>, CH<sub>4</sub> and N<sub>2</sub>O were measured with a Dual Laser Trace Gas Analyzer (TILDAS, Aerodyne Research, Billerica, USA) since 2017. Since January 2021, these measurements were reduced to measure CH<sub>4</sub> only, due to failure of one of the lasers. In addition, since November 2019, CO<sub>2</sub> concentrations in the chambers were measured with an  
100 infrared gas analyzer (LI-840, LI-COR Biosciences, Lincoln NE, USA). For the year 2020, CO<sub>2</sub> chamber measurements from both QCL and LIL-840 were available and used for further analyses. Chambers were designed according to Brümmer et al. (2017), following the ICOS RI protocol for chamber measurements (Pavelka et al., 2018). The opaque PVC chambers rested on aluminum frames, inserted 10 cm in the soil, sealed with EPDM (ethylene propylene diene monomer) gaskets, and had the dimension of 75 cm x 75 cm x 50 cm height (thus approx. 281 dm<sup>3</sup>). They were equipped with a pressure vent, as well as air  
105 temperature and pressure sensors (BME280, Bosch Sensortec GmbH, Reutlingen, Germany). During the winter periods with snowfall, extension frames (2 x 50 cm height) allowed to increase their height. A 17 Watt geared electric motor (80807021, Crouzet, Valence, France) was used to move the entire PVC chamber vertically and horizontally by about 190 cm and 70 cm, respectively. One webcam per chamber allowed remote observation of the operation and estimate of snow cover and depth (see below). Since the vegetation inside the chamber frames was not cut, the chamber set-up measured forest-floor GHG fluxes  
110 (and not only soil fluxes). Due to their opaque material, no understory photosynthesis was measured with the chambers. Soil and vegetation cover inside the chambers (differentiated into three plant functional types: moss, grass, blueberry) were assessed visually in June 2022, when also the leaf area index (LAI) of the spruce forest was measured using digital photography above the chamber locations (Fuentes et al., 2008). One chamber cycle fit within 10 minutes, including closing and opening operations (controlled by an Arduino Ethernet), with an actual measurement period of 180 s when the chamber resided on the  
115 frame. The air from the chamber was fed to the gas analyzers in 6 mm OD tubing (Synflex 1300, Eaton, Dublin, Ireland) and pumped back to the chamber, forming a closed system. Switching of the air stream between the different chambers and the gas analyzers was accomplished using rotary selector valves (Valco Selectors, VICI AG International, Schenkon, Switzerland). Chamber cycles (lasting app. 1 h for four chambers) were repeated every 3 hours for each gas analyzer individually, leading to total 16 cycles per chamber and day (eight per gas analyzer). Chambers leakage tests of all four chambers were performed  
120 in 2019. Variations caused by possible leakage were below 3% of the measured flux, as required by the ICOS RI protocol (Pavelka et al., 2018).

**Tab. 1: Site characteristics of the four chambers (FF1 to FF4). Annual means and standard deviations are shown for soil temperature ( $T_{\text{soil}}$ ) and water filled pore space (WFPS) at 5 cm, soil depth, and days with snow cover. LAI, soil, and vegetation cover inside each**



125 chamber were determined in June 2022. Soil data (bulk density, pH, C and N stocks in the topsoil, i.e., litter, organic material layers, and 0–20 cm depth of mineral soil) were taken from Jörg (2008).

Site characteristics	FF1	FF2	FF3	FF4	Mean
<b>T<sub>soil</sub> at 5 cm (°C)</b>					
2017	4.44 ± 4.67	4.16 ± 4.84	4.29 ± 4.86	4.56 ± 4.52	4.36 ± 0.17
2020	4.66 ± 4.32	4.40 ± 4.46	4.46 ± 4.34	4.87 ± 4.15	4.60 ± 0.22
2021	4.18 ± 4.25	3.80 ± 4.48	3.74 ± 4.84	4.26 ± 4.20	3.99 ± 0.26
2022	5.15 ± 4.70	4.83 ± 4.96	4.70 ± 5.38	5.18 ± 4.61	4.97 ± 0.24
<b>WFPS at 5 cm (%)</b>					
2017	20.1 ± 5.09	17.2 ± 4.30	21.3 ± 6.82	22.5 ± 7.42	20.3 ± 2.27
2020	15.9 ± 2.88	15.5 ± 3.85	9.8 ± 0.69	23.9 ± 9.55	16.3 ± 5.79
2021	16.8 ± 3.88	14.5 ± 3.88	11.8 ± 4.45	25.0 ± 10.5	17.0 ± 5.70
2022	15.1 ± 4.19	12.7 ± 3.27	10.4 ± 3.56	21.3 ± 7.16	14.9 ± 4.70
<b>Snow depth (cm)</b>					
2017	5.8 ± 8.4	6.4 ± 9.8	4.5 ± 6.4	3.9 ± 6.2	5.1 ± 1.2
2020	4.3 ± 7.0	8.6 ± 12.1	4.2 ± 7.0	3.5 ± 6.0	5.2 ± 2.3
2021	17.6 ± 25.0	22.2 ± 29.5	14.6 ± 22.7	14.8 ± 21.0	17.3 ± 3.6
2022	5.1 ± 9.3	8.3 ± 14.1	6.1 ± 11.7	4.9 ± 9.5	6.1 ± 1.6
<b>Days with snow cover</b>					
2017	152	159	152	148	153 ± 5
2020	126	142	123	117	127 ± 11
2021	172	189	161	169	173 ± 12
2022	138	145	134	132	137 ± 6
Leaf area index (LAI)	2.9	4.2	3.1	2.9	3.3 ± 0.6
<b>Soil cover inside chamber (%)</b>					
bare soil	0	50	70	0	30 ± 36
moss	90	50	20	90	63 ± 34
grass	5	1	0	0	2 ± 2
<i>Vaccinium</i>	60	0	10	30	25 ± 26
Bulk density at 5 cm (g cm <sup>-3</sup> )	0.27	0.35	0.32	0.35	0.32 ± 0.04
pH	2.8–3.1	3.0–3.4	2.8–3.1	3.0–3.4	
C stock (t/ha)	93.5	147.7	135.4	105.8	120.6 ± 25.2
N stock (t/ha)	3.54	5.74	4.47	3.52	4.32 ± 1.05

### 2.2.2 Data processing and quality assessment

The concentration increase in the chamber headspace over time was used to determine the respective flux  $F$  using Eq. (1):

$$130 \quad F = \frac{\frac{\partial c}{\partial t} V \frac{m}{A} \frac{p}{V_m} \frac{T_0}{p_0} \frac{T}{T_0}}{m} \quad (1)$$

where  $\frac{\partial c}{\partial t}$  is the concentration change over time (mol mol<sup>-1</sup> s<sup>-1</sup>),  $V$  the actual chamber volume (m<sup>3</sup>),  $A$  the forest-floor area within the chamber frame (m<sup>2</sup>),  $m$  the molecular mass (dimensionless),  $V_m$  the molar volume (m<sup>3</sup> mol<sup>-1</sup>) of the respective gas,



$p$  the mean chamber pressure (Pa),  $p_0$  the standard pressure (1013.25 Pa),  $T_0$  the standard temperature (273.15 K), and  $T$  the mean chamber temperature (K). We fitted a linear regression to the change in concentration of the respective gas over time  
 135  $(\frac{\partial C}{\partial t})$  during the closed period of the chamber (180 s), excluding the first 20 s after closing. The  $R^2$  of the fit was later used for the quality assessment and filtering of the calculated fluxes (see below). A positive flux means release from the forest floor to the atmosphere, and a negative flux indicates uptake by the forest floor.

The quality of the calculated fluxes was ensured by removing negative  $\text{CO}_2$  fluxes (Step 1), removing outliers (Step 2, despiking), and applying a filter based on  $R^2$  (Step 3). (1) We excluded any negative  $\text{CO}_2$  fluxes (about 2 % of all fluxes). (2)  
 140 We then despiked the flux data set with a running mean algorithm using a width of 30 days. (3) For the growing period (May to November) and the dormant period (December to April) separately, we removed fluxes with a  $R^2$  value below the 10<sup>th</sup> percentile of all  $R^2$  values in the respective period (except if  $R^2 > 0.9$ ), to avoid setting a fixed threshold for an acceptable  $R^2$ . These three steps were applied to each chamber and GHG separately. The 10<sup>th</sup> percentile of  $R^2$  values ranged from 0.001 to 0.99, being lower during the dormant compared to the growing period and particularly for  $\text{N}_2\text{O}$  fluxes (Tab. 2).

145

**Tab. 2: 10<sup>th</sup> percentiles of  $R^2$  values from linear regressions used for flux calculations per gas, given separately for each chamber (FF1 to FF4) and growing and dormant periods. Percentiles were applied as quality thresholds.**

Gas	Period	FF1	FF2	FF3	FF4
$\text{CO}_2$	growing period	0.97	0.98	0.98	0.99
	dormant period	0.35	0.48	0.47	0.68
$\text{CH}_4$	growing period	0.92	0.96	0.92	0.93
	dormant period	0.41	0.26	0.21	0.61
$\text{N}_2\text{O}$	growing period	0.022	0.001	0.001	0.003
	dormant period	0.042	0.002	0.003	0.002

Initially, the time series consisted of 40'426  $\text{CO}_2$  (in 2020 from both gas analyzers), 31'998  $\text{CH}_4$  and 14'309  $\text{N}_2\text{O}$  flux  
 150 measurements over the four years. After the quality checks described above, 37'596  $\text{CO}_2$  (93 %) and 26'565  $\text{CH}_4$  (83 %) flux measurements remained, which resulted in 4446 and 3972 daily means, respectively. Due to Step 3, we excluded the forest-floor  $\text{N}_2\text{O}$  fluxes from further driver and budget analyses.

### 2.3 Environmental data

Each of the chambers had measurements of soil water content (SWC; EC-5, Decagon Devices Inc.) and  $T_{\text{soil}}$  (107, Campbell  
 155 Scientific Ltd.) at 5 cm soil depth in close vicinity (< 2 m away from the chamber). To account for potential drivers of canopy photosynthesis modulating forest-floor fluxes, photosynthetic photon flux density (PPFD; PAR LITE, Kipp & Zonen), air temperature (TA; HygroClip HC2-S3, Rotronic AG), and precipitation (PREC; 1518H3, Lambrecht Meteo GmbH) data were used as well, measured at the tower above the tree canopy at 35 m height (precipitation at 25 m height).

We calculated water-filled pore space (WFPS) from the soil water content (SWC) measurements using Eq. (2):



160 
$$WFPS = \frac{SWC}{1 - \frac{BD}{PD}} \times 100 \quad (2)$$

Bulk density (BD) was calculated using the data from a soil sampling campaign done in July 2018 according to ICOS RI standards (Arrouays et al., 2018). Soil data were used from soil profiles closest to the respective chambers (in total, data from six profiles were used). Particle density (PD) was assumed to be constant at 2.65 g cm<sup>-3</sup> (Danielson and Sutherland, 2018). The mean daily snow cover and snow depth per chamber was derived from webcam images using a custom-made python  
165 image analysis tool, deriving snow depth from a scale installed in vicinity to each chamber within the image section.

## 2.4 Statistical analyses

### 2.4.1 Driver analysis

We used conditional random forests (RF) to model daily forest-floor CO<sub>2</sub> and CH<sub>4</sub> fluxes (based on all years and chambers) and investigate their environmental drivers. We selected predictors which were known from the literature, i.e., daily averages  
170 of T<sub>air</sub>, T<sub>soil</sub> at 5 cm depth, WFPS at 5 cm depth, and PPFD as well as their one- and four-day leads (meaning that we shifted the variables forward in time by one and four days). Furthermore, we added snow depth and changes in snow depth from one day to another (Δ snow depth) to the predictor set. To account for factors which could explain differences in the GHG fluxes among the chambers, we included several chamber-specific characteristics (Tab. 1), i.e., the LAI, the bare soil fraction in the chambers, and the total C and N stocks in the topsoil (litter, organic material layers, and 0–20 cm depth of mineral soil). We  
175 applied the function *cforest* from the R-package “party” which can deal with highly correlated predictor variables (v1.3.10; Strobl et al., 2008, 2007). Prior to model development, predictors and target variables were centered and scaled using the “caret” *preProcess* function, which brings all variables and measurements from different sensors and locations into the same range improving performance of the RF models (v6.0.93; Kuhn, 2008). The hyperparameter fitting was done using the train function from the R-package “caret” (see Appendix for final model setup) using 10-fold cross-validation. The assessment of  
180 driver importance in the RF model was done using the R package “permimp” which accounts for correlated variables within the predictor set (v.1.0.2; Strobl et al., 2007; Debeer and Strobl, 2020; Debeer et al., 2021). The calculated values for driver importance were rescaled to values between 0 and 1 using a min-max normalization.

We developed RF models separately for daily CO<sub>2</sub> and CH<sub>4</sub> fluxes (N = 4446 and 3972, respectively). The training of the RF was done using only a fraction of the data set (70 %). The remaining 30 % of the data set was used as test dataset to evaluate  
185 model performance. Centering and scaling were done separately for training and test datasets to avoid data leakage. The performance of the RF models was assessed using R<sup>2</sup> and random mean square errors (RMSE). During model development, we tested several different predictor sets. Furthermore, to optimize the models and to evaluate the robustness of model results, we evaluated the RF models trained on data sets separated by year of measurement or by chamber, and compared their accuracy to the model that was built using data from all years and all chambers. In total, 17 predictor variables entered the models  
190 (including the leads). RF models were also trained on seasonal data (i.e., spring, summer, autumn, winter; defined according to the meteorological definition) to investigate differences in drivers among the seasons. For the seasonal RFs, we used the



same predictor sets as for the RFs developed on the entire data set. We calculated partial dependence (PD) plots of the conditional RFs using the “moreparty” package (v0.3.1; Robette, 2023) which is based on the “pdp” package (v0.8.1; Goldstein et al., 2015; Greenwell, 2017) to assess the relationships between the four most important predictors and the predictions. The PD is calculated as the change in the average predicted value, while the predictor at interest is varied over its marginal distribution.

## 2.4.2 Flux gap-filling and budget calculation

The gap-filling of CO<sub>2</sub> and CH<sub>4</sub> fluxes was done using the RF models developed above. Missing values in the predictor variables (gap length < 3 days) were linearly interpolated using the R package “chillR” (v0.72.8, Luedeling and Fernandez, 2022). The gap-filled flux data were then used to calculate the annual forest-floor GHG budgets per chamber. Since we estimated the annual forest-floor GHG budget for the study area, we report the mean over the four chambers. To be able to compare CO<sub>2</sub> and CH<sub>4</sub> budgets, we converted the CH<sub>4</sub> budgets into CO<sub>2</sub>-equivalents (CO<sub>2</sub>-eq) using the 100-year global warming potential of methane of 27 (IPCC, 2021).

In addition, we modeled the daily CO<sub>2</sub> fluxes using a Q<sub>10</sub> model according to Eq. (3):

$$R_S = R_{ref} \times Q_{10}^{\frac{T_{soil} - 10}{10}} \quad (3)$$

where R<sub>ref</sub> is the modeled R<sub>S</sub> at a T<sub>soil</sub> of 10°C, and Q<sub>10</sub> is the temperature sensitivity. We developed one model for the full dataset (all years and all four chambers together). The annual budgets calculated with the Q<sub>10</sub> modeled fluxes were then compared to the annual budgets from the RF gap-filling. All statistical analyses were performed using R Statistical Software (v4.2.0, R Core Team, 2022).

## 210 3 Results

### 3.1 Seasonal and interannual variability of environmental conditions and GHG fluxes

The seasonal courses of T<sub>air</sub> and T<sub>soil</sub> were very pronounced during the four years of the study, with highest temperatures in July and August, and lowest temperatures in January (Fig. 1a). All years showed highly variable WFPS with large differences among chambers (i.e., up to 35 % difference; Fig. 1b), with highest values during the snowmelt period, i.e., March to May. While the snow-covered periods usually started in November and lasted until April or May (Fig. 1c), the snow depths were much higher during winter 2020/2021 (reaching snow depths of over 1 m) compared to the other winters. Overall, the year 2022 was by far the warmest year ever recorded at the Davos research site, with an annual mean T<sub>air</sub> of 5.6 °C (vs. the long-term mean of 4.3 °C; station data 1997–2022). Accordingly, annual mean T<sub>soil</sub> at 5 cm was highest in 2022 for all chambers (annual mean T<sub>soil</sub> over all chambers was 5.0 °C; Tab. 1). At the same time, precipitation in 2022 was low (773 mm vs. long-term mean of 876 mm; station data 1997–2022), which led to comparably dry soil conditions (annual mean WFPS over all chambers was lowest in 2022 (14.9 %) compared to that of the other years).





On the one hand, the forest floor at the Davos Seehornwald site was a source of CO<sub>2</sub> during all four years, independent of the season (Fig. 1d). Typically, forest-floor CO<sub>2</sub> fluxes were very low in winter (mean CO<sub>2</sub> flux ± standard deviation (SD): 0.46±0.14 μmol m<sup>-2</sup> s<sup>-1</sup>), increased in spring after the snow melt, and reached their maximum values in June to September (mean CO<sub>2</sub> flux over all years: 3.50±0.84 μmol m<sup>-2</sup> s<sup>-1</sup>). Lowest forest-floor CO<sub>2</sub> emissions were measured in January 2021 (min. CO<sub>2</sub> flux: 0.06 μmol m<sup>-2</sup> s<sup>-1</sup>), highest CO<sub>2</sub> fluxes were observed in July 2022 (max. CO<sub>2</sub> flux: 6.54 μmol m<sup>-2</sup> s<sup>-1</sup>).

On the other hand, the forest floor was a consistent sink for CH<sub>4</sub>, despite large short-term variations (days to weeks; Fig. 1e) and a few short peaks of CH<sub>4</sub> emissions in winter and spring. Seasonality of forest-floor CH<sub>4</sub> fluxes was very pronounced, with highest uptake in summer (mean CH<sub>4</sub> flux: -2.11±0.28 nmol m<sup>-2</sup> s<sup>-1</sup>), and still high CH<sub>4</sub> uptake rates during autumn and early winter (October to December; most clearly seen in 2022). Lowest CH<sub>4</sub> uptake was measured in the months of February to March (mean CH<sub>4</sub> flux: -0.44±0.22 nmol m<sup>-2</sup> s<sup>-1</sup>). With increasing duration of winter (March to May; Fig. 1e), the CH<sub>4</sub> sink strength further decreased. However, at the end of winter, between April and end of May (depending on the year), CH<sub>4</sub> uptake rates increased sharply.

Based on quality check 3, we did not consider the N<sub>2</sub>O fluxes any further. The decision was driven by the observed low 10<sup>th</sup> percentiles of the R<sup>2</sup> values (Tab. 2), which indicated that the flux calculations frequently failed to yield satisfactory fits due to very low forest-floor N<sub>2</sub>O fluxes (Appendix Fig. A.1), often below the minimum detectable flux of N<sub>2</sub>O. This minimum reliable flux was estimated with the specifications of the TILDAS instrument (precision of 0.03 ppb), i.e., any change of N<sub>2</sub>O concentrations in the chamber headspace during the measurement period had to be > 0.06 ppb (McManus et al., 2006) or > 29.1 nmol N<sub>2</sub>O m<sup>-2</sup> h<sup>-1</sup>.

240

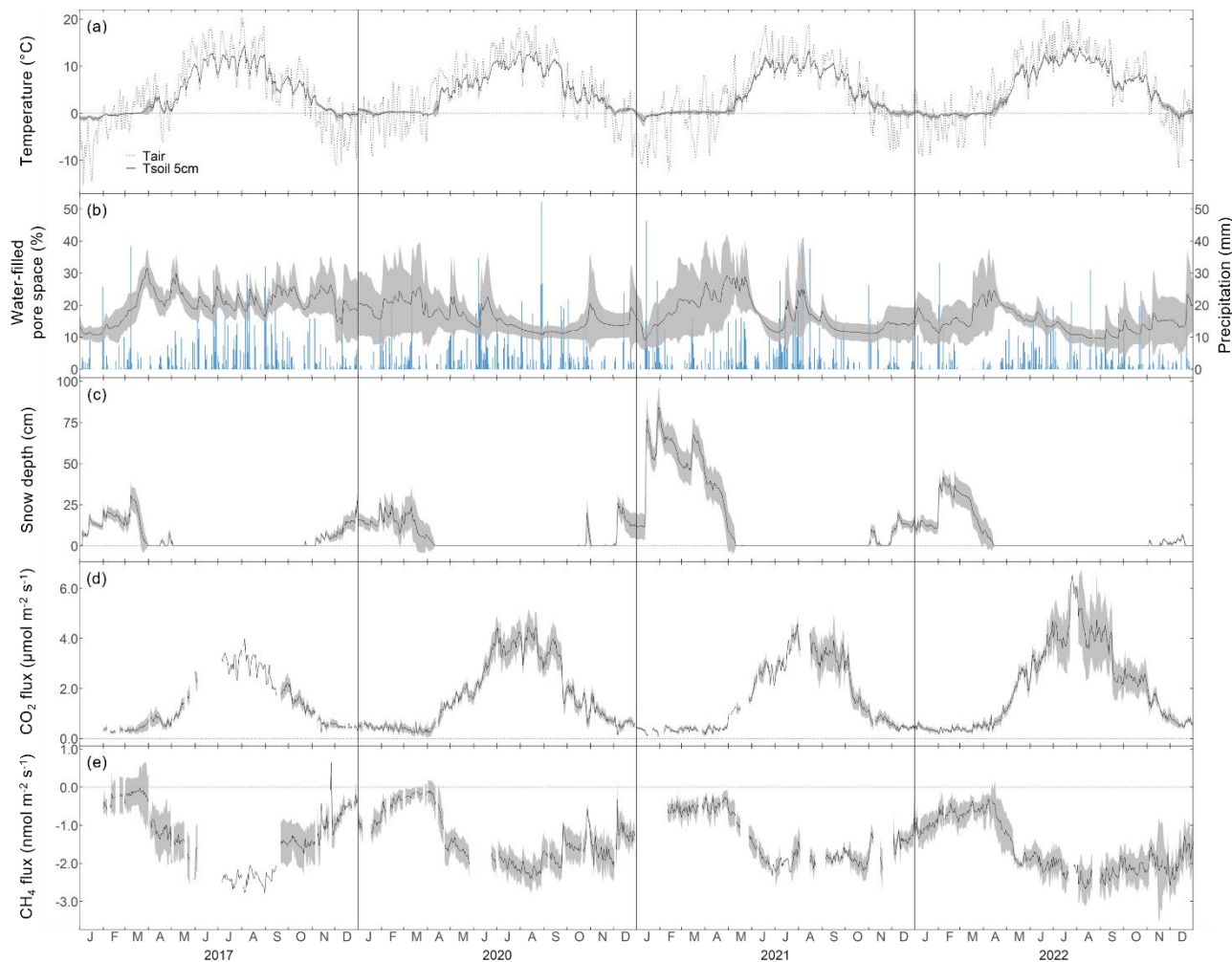


**Fig. 1:** Daily mean a) air temperature and soil temperature at 5 cm depth, b) water-filled pore space at 5 cm depth (left axis) and daily sum of precipitation (right axis), c) snow depth, and daily mean forest-floor d) CO<sub>2</sub> fluxes (not gap-filled), and e) CH<sub>4</sub> fluxes (not gap-filled), for the years 2017, 2020, 2021, and 2022. Black lines show means over four chambers, grey bands show standard deviations among four chambers. All data shown were quality-checked as described in the main text.

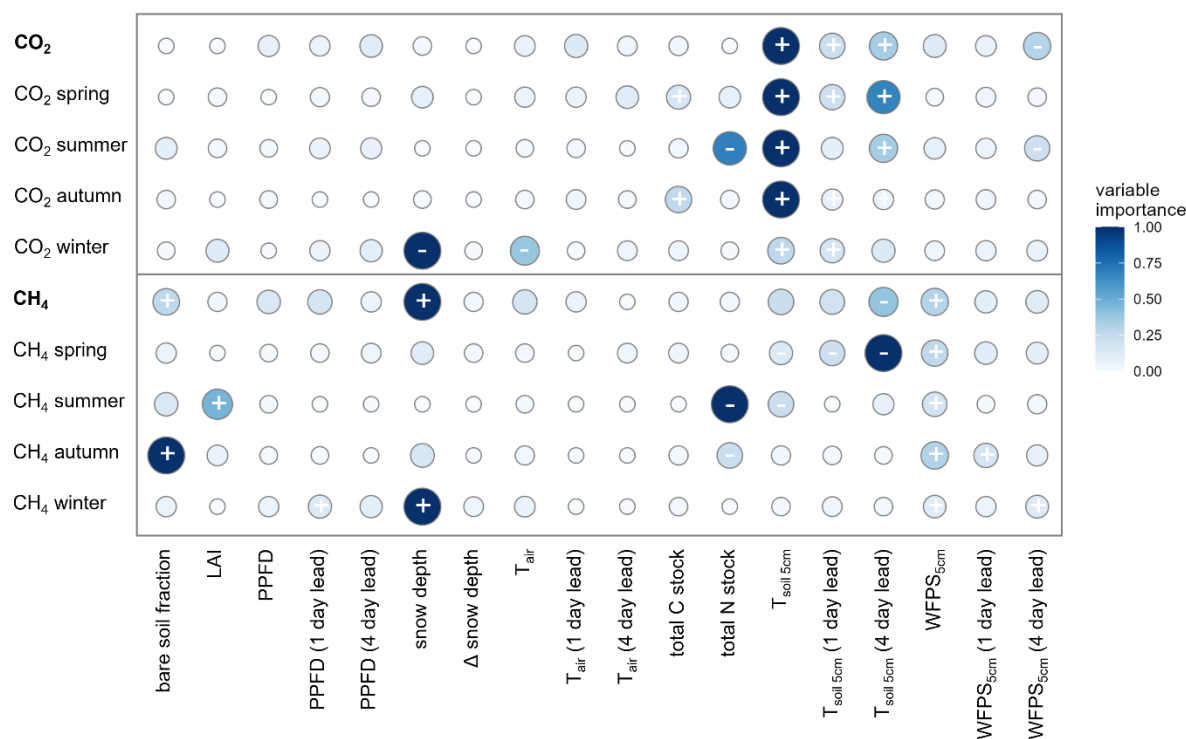
245

### 3.2 Driver analyses with random forest models

The RF models captured the temporal dynamics and absolute magnitudes of the observed forest-floor CO<sub>2</sub> and CH<sub>4</sub> fluxes very well, with R<sup>2</sup> values of 0.95 and 0.87, respectively (relationships of observed vs. predicted fluxes from test datasets) and RSME of 0.32 µmol m<sup>-2</sup> s<sup>-1</sup> and 0.27 nmol m<sup>-2</sup> s<sup>-1</sup>, respectively (Fig. A.2). Also the seasonal RF models for forest-floor CO<sub>2</sub> fluxes yielded high R<sup>2</sup> values of 0.94, 0.73, 0.90 and 0.63 for spring, summer, autumn and winter, respectively (Tab. A.1).



255 Similarly, forest-floor CH<sub>4</sub> fluxes during spring, summer, autumn and winter were predicted well, with R<sup>2</sup> values of 0.80, 0.76, 0.72 and 0.73, respectively. Thus, the RF model performance was very good, also when shorter time periods were considered. Forest-floor CO<sub>2</sub> fluxes combined for all four years and seasons were predominantly driven by T<sub>soil</sub> at 5 cm depth: T<sub>soil</sub> at the time of the flux measurements was the most important driver, but also T<sub>soil</sub> with a four-day (second most important) and with a one-day lead were relevant (Fig. 2). Furthermore, WFPS at 5 cm with a four-day lead played an important role. As expected, higher T<sub>soil</sub> lead to higher CO<sub>2</sub> emissions, while higher WFPS reduced CO<sub>2</sub> emissions. No emissions of drivers enhancing canopy photosynthesis, i.e., LAI or PPFD, were observed. Separating the forest-floor CO<sub>2</sub> fluxes into seasonal fluxes resulted in a clear distinction of drivers in winter compared to the other seasons (Fig. 2). Winter CO<sub>2</sub> fluxes were mainly driven by  
260 snow depth (most important driver; higher snow depth leading to lower CO<sub>2</sub> fluxes), while T<sub>soil</sub> played a smaller role. As for the overall fluxes, summer forest-floor CO<sub>2</sub> fluxes were mainly driven by T<sub>soil</sub>, but also total N stocks were highly relevant (higher total N stock leading to lower CO<sub>2</sub> fluxes), much in contrast to the fluxes during spring and fall (Fig. 2).



265 **Fig. 2: Relative variable importance (rescaled to 0–1) according to the random forest driver analysis for CO<sub>2</sub> (top) and CH<sub>4</sub> (bottom) fluxes (not gap-filled; shown for the entire year, and per season). The direction of the effect of each predictor variable on the fluxes is shown by + (positive correlation) and – (negative correlation) signs, i.e., + indicates increased CO<sub>2</sub> emissions or decreased CH<sub>4</sub> uptake (increased CH<sub>4</sub> emissions). Signs are given for the four most important predictors which was investigated using partial dependence plots. See Materials and Methods for variable abbreviations.**

270

Forest-floor CH<sub>4</sub> fluxes combined for all four years and seasons were mainly driven by the snow depth (higher snow depth leading to more positive CH<sub>4</sub> fluxes and thus less CH<sub>4</sub> uptake; Fig. 2). Furthermore, the four-day lead of T<sub>soil</sub> at 5 cm, WFPS at 5 cm, and the bare soil fraction inside the chamber strongly impacted the fluxes. We found that the drivers of the forest-floor CH<sub>4</sub> fluxes changed profoundly among seasons. Spring CH<sub>4</sub> fluxes were mainly temperature-driven (higher temperatures leading to more CH<sub>4</sub> uptake). In summer, forest-floor CH<sub>4</sub> fluxes were mainly driven by total N stocks (higher N stocks leading to more negative CH<sub>4</sub> fluxes and thus higher uptake) and by LAI (higher LAI leading to more positive CH<sub>4</sub> fluxes and thus lower uptake), reflecting spatial variability among chambers. In addition, CH<sub>4</sub> fluxes were influenced by an interaction of several drivers such as T<sub>soil</sub> (higher T<sub>soil</sub> leading to higher uptake) and WFPS (higher WFPS leading to lower uptake). For autumn CH<sub>4</sub> fluxes, bare soil fraction was the most important driver (more bare soil – and thus smaller moss cover (Tab. 1) – leading to more positive CH<sub>4</sub> fluxes and thus less CH<sub>4</sub> uptake), but also WFPS played an important role. Winter CH<sub>4</sub> fluxes responded mainly to snow depth (higher snow depth leading to less CH<sub>4</sub> uptake; Fig. 2).

280



### 3.3 Forest-floor CO<sub>2</sub> and CH<sub>4</sub> budgets

The forest floor of this subalpine spruce forest was a net source of CO<sub>2</sub> and a net sink of CH<sub>4</sub> for all years of the study (averaged over all four chambers; Tab. 3). Mean annual forest-floor CO<sub>2</sub> and CH<sub>4</sub> budgets were 2.33±0.20 kg CO<sub>2</sub> m<sup>-2</sup> yr<sup>-1</sup> and -0.71±0.06 g CH<sub>4</sub> m<sup>-2</sup> yr<sup>-1</sup>, respectively. The annual forest-floor CO<sub>2</sub> budgets were mainly determined by summer and early autumn fluxes (i.e., June to September). The interannual variability (SD) of forest-floor CO<sub>2</sub> budgets was approx. 0.2 kg CO<sub>2</sub> m<sup>-2</sup> yr<sup>-1</sup> (8.6 %) during the four years of the study, with 2017 and 2021 showing smaller and 2022 the highest emissions. The annual CO<sub>2</sub> budgets calculated with the Q<sub>10</sub> modeled data (2.42±0.21 kg CO<sub>2</sub> m<sup>-2</sup> yr<sup>-1</sup>; Tab. 3) agreed well with the CO<sub>2</sub> budgets based on the gap-filled fluxes using RF, also showing highest fluxes in 2022. A similar interannual variability (SD) as for the CO<sub>2</sub> budgets was found for the CH<sub>4</sub> budgets, with 8.5 % (0.06 g CH<sub>4</sub> m<sup>-2</sup> yr<sup>-1</sup>). Comparing the magnitudes of the forest-floor CO<sub>2</sub> and CH<sub>4</sub> budgets (in CO<sub>2</sub>-eq) clearly showed that the CO<sub>2</sub> budget determined the forest-floor GHG budget of the spruce forest, since the CH<sub>4</sub> uptake (-19.1 g CO<sub>2</sub>-eq m<sup>-2</sup> yr<sup>-1</sup>) was about two orders of magnitude smaller than the CO<sub>2</sub> emissions (2336±200 g CO<sub>2</sub>-eq m<sup>-2</sup> yr<sup>-1</sup>).

**Tab. 3: Mean annual budgets (±standard deviation (SD) over four chambers) of CO<sub>2</sub> and CH<sub>4</sub> forest-floor fluxes (using gap-filled data). The Q<sub>10</sub> budget was calculated with Eq. 3 (Q<sub>10</sub> and R<sub>ref</sub> estimates were 4.8 and 3.16, respectively; overall R<sup>2</sup> was 0.86).**

Year	CO <sub>2</sub> budget		Q <sub>10</sub> budget (g CO <sub>2</sub> m <sup>-2</sup> yr <sup>-1</sup> )	CH <sub>4</sub> budget		(g CH <sub>4</sub> m <sup>-2</sup> yr <sup>-1</sup> )	Net GHG budget (g CO <sub>2</sub> -eq m <sup>-2</sup> yr <sup>-1</sup> )
	(g CO <sub>2</sub> m <sup>-2</sup> yr <sup>-1</sup> )	(g C m <sup>-2</sup> yr <sup>-1</sup> )		(g CO <sub>2</sub> -eq m <sup>-2</sup> yr <sup>-1</sup> )	(g C m <sup>-2</sup> yr <sup>-1</sup> )		
2017	2139±334	584± 91	2407±28	-17.1±3.6	-0.47±0.10	-0.63±0.13	2122±334
2020	2338±324	638± 89	2390±54	-18.7±3.3	-0.52±0.09	-0.69±0.12	2319±324
2021	2138±275	584± 75	2204±40	-18.3±2.7	-0.51±0.08	-0.68±0.10	2120±275
2022	2730±589	745±161	2687±40	-22.2±4.4	-0.62±0.12	-0.82±0.16	2708±579
Overall	2336±200	638±55	2422±21	-19.1±1.8	-0.53±0.05	-0.71±0.06	2317±200

The year 2022 can be considered an exceptional year, both in terms of annual forest-floor CO<sub>2</sub> and CH<sub>4</sub> fluxes (Tab. 3), but also in terms of temporal development (Fig. 3a). For CO<sub>2</sub>, there were not only higher emission rates in summer, but also a faster increase in CO<sub>2</sub> emission rates already in mid-April and sustained higher emissions until later in the year (Fig. 3a). The exceptionally high CO<sub>2</sub> fluxes coincided with the higher-than-usual T<sub>soil</sub> which was the main driver of spring, summer, and autumn CO<sub>2</sub> fluxes. For CH<sub>4</sub>, we observed a considerably higher annual CH<sub>4</sub> uptake in 2022 compared to other years (Tab. 3), mainly due to higher uptake rates in summer as well as still high uptake rates in autumn and early winter (Fig. 3b). Apart from higher T<sub>soil</sub> driving the higher summer CH<sub>4</sub> uptake, this was mainly connected to comparably low soil moisture in autumn 2022 and the exceptionally low snow amount in November and December 2022.

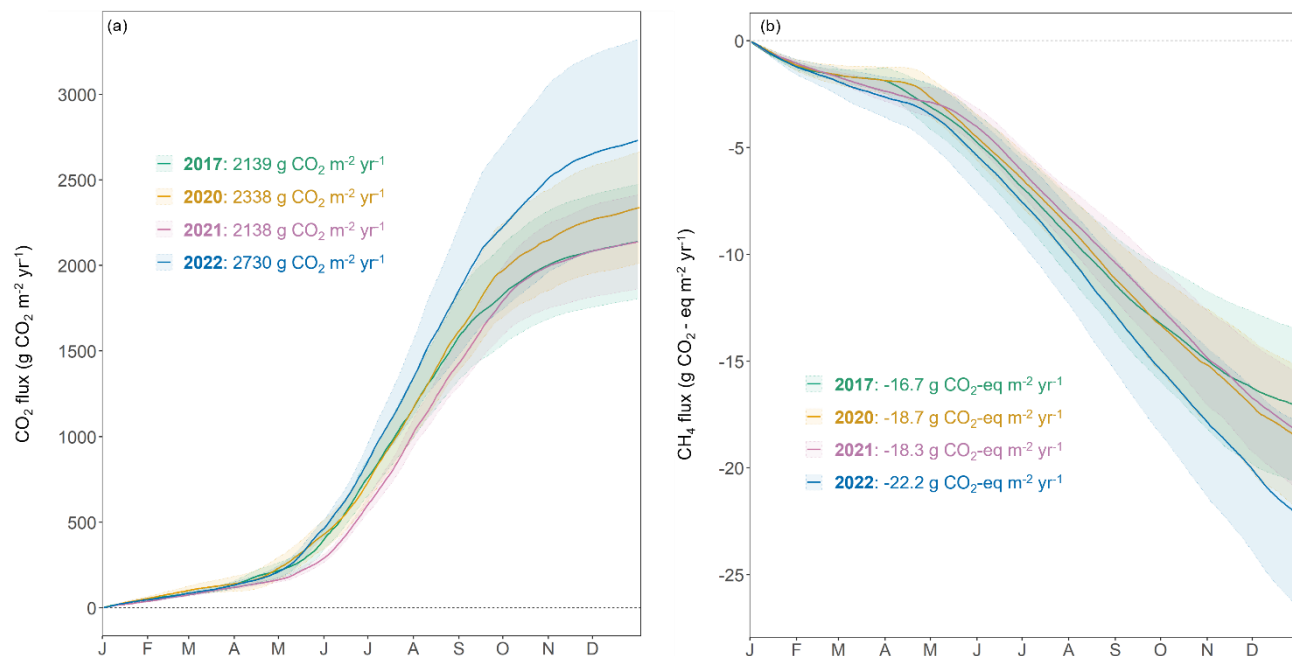


**Fig. 3: Cumulative (a) CO<sub>2</sub> (g CO<sub>2</sub> m<sup>-2</sup> yr<sup>-1</sup>) and (b) CH<sub>4</sub> (g CO<sub>2</sub>-eq m<sup>-2</sup> yr<sup>-1</sup>) forest-floor fluxes over four years. Lines show means of all four chambers; colored bands represent standard deviations among four chambers.**

## 310 4 Discussion

### 4.1 Interannual variability in forest-floor GHG fluxes

Over the four-year measurement period (2017 and 2020–2022), we acquired high-resolution forest-floor GHG flux data for four distinct years allowing comprehensive year-round analyses. Notably, 2022 emerged as the warmest year ever recorded at the Davos site, coinciding with remarkably low precipitation levels. Despite these counteracting environmental conditions, forest-floor CO<sub>2</sub> emissions in 2022 exceeded the other three years by approximately 20 %. Concurrently, we observed the highest forest-floor CH<sub>4</sub> uptake in 2022. Anjileli et al. (2021) reported that even during extreme heat events soil respiration increased by approximately 25 % compared to average conditions, emphasizing the dominating influence of temperature on CO<sub>2</sub> emissions also under extreme dry conditions. Additionally, Borcken et al. (2006) indicated that droughts can enhance the soil CH<sub>4</sub> sink in temperate forests. In contrast, the year 2021 was the coldest year among the four years we investigated, with an annual mean T<sub>air</sub> of 3.9 °C mainly driven by below-average spring temperatures. This was reflected clearly in the GHG fluxes with below-average CO<sub>2</sub> emissions (approximately 30 % lower compared to the four-year mean) and below-average CH<sub>4</sub> uptake in spring 2021 (approximately 20 % lower compared to the four-year mean). Moreover, 2021 was an exceptional year in terms of snow amount (snow depth in winter and spring exceeded the four-year average by 87 % and 145 %, respectively), relevant drivers identified in this study.



325 While the year 2020 was also characterized by a warm weather, its summer temperatures were less extreme than those in 2022. Our findings revealed that the CO<sub>2</sub> emissions in 2020 did not reach the levels observed in 2022, supporting our driver analyses, clearly indicating that the exceptionally high summer temperatures experienced in 2022 were the primary driving force behind the 2022 annual CO<sub>2</sub> emissions. The RF models for 2022 resulted in slightly lower forest-floor CO<sub>2</sub> fluxes than measured, suggesting that no overfitting had occurred (Fig. A.3, A.4). Moreover, these results highlight the critical role played by extreme  
330 summer temperatures in shaping the C dynamics of this subalpine spruce ecosystem and underscore the significance of understanding their implications for future C budgets, potentially reducing the overall C sink behavior observed so far in this forest (Zielis et al., 2014).

#### 4.2 Drivers of forest-floor GHG fluxes

Forest-floor GHG fluxes were shown to have very distinct drivers across the different season. Consistent with our expectations, soil temperature predominantly controlled forest-floor CO<sub>2</sub> fluxes, thereby influencing the annual CO<sub>2</sub> budget at annual as  
335 well as seasonal scales (except winter season). In contrast, no effects of drivers known to enhance canopy photosynthesis (i.e., LAI, PPFD) and thus below-ground allocation and soil respiration (Högberg et al., 2001) were observed on the forest-floor CO<sub>2</sub> fluxes for any time in this spruce forest, suggesting a strong direct control of environmental factors and a weak or even lacking indirect control of canopy biology. Drivers of forest-floor CH<sub>4</sub> fluxes were much more variable compared to those for  
340 CO<sub>2</sub> fluxes, with winter CH<sub>4</sub> fluxes being affected by the same driver (snow depth) as the annual fluxes. In addition, CH<sub>4</sub> fluxes responded most strongly to WFPS in autumn. These findings support the hypothesis proposed by Borken et al. (2006), which emphasized the role of factors influencing the diffusion rates of atmospheric CH<sub>4</sub> into the soil, such as soil water content and snow cover, in determining CH<sub>4</sub> uptake in forest soils. Notably, previous studies have also reported a close relationship between CH<sub>4</sub> fluxes and seasonal changes in soil moisture (Ni and Groffman, 2018; Ueyama et al., 2015). However, our results  
345 indicated that in spring and summer, T<sub>soil</sub> rather than WFPS played a more important role in driving forest-floor CH<sub>4</sub> uptake. Additionally, we identified a notable influence of soil N on summer CH<sub>4</sub> fluxes, with higher N stocks, and thus most likely higher N mineralization during the summer months, corresponding to enhanced CH<sub>4</sub> uptake. This aligns with previous findings in forest ecosystems, where soil mineral N has been shown to stimulate CH<sub>4</sub> oxidation (Goldman et al., 1995; Martinson et al., 2021). Moreover, we found a positive correlation between bare soil fraction and forest-floor CH<sub>4</sub> uptake, i.e., less bare soil  
350 and thus higher moss cover leading to higher forest-floor CH<sub>4</sub> uptake. This is in line with the findings that *Sphagnum* mosses can promote CH<sub>4</sub> oxidation (Basiliko et al., 2004). Also for forest-floor CH<sub>4</sub> fluxes, hardly any effect of canopy biology was detected (except for summer). Thus, a strong direct control of environmental factors on both GHG fluxes was observed, increasing the vulnerability of the forest C sink with future climate change (IPCC, 2021).

#### 4.3 Forest-floor GHG budgets

355 The overall forest-floor GHG budget showed a total emission of 2317±200 g CO<sub>2</sub>-eq m<sup>-2</sup> yr<sup>-1</sup>, dominated by the annual CO<sub>2</sub> budget (2.34±0.20 kg CO<sub>2</sub> m<sup>-2</sup> yr<sup>-1</sup>), which was within the range of studies conducted in temperate, subalpine or boreal forests



which we consider comparable to our site ( $1.07\text{--}2.91 \text{ kg CO}_2 \text{ m}^{-2} \text{ yr}^{-1}$ ; Gaumont-Guay et al., 2014; Groffman et al., 2006; Schindlbacher et al., 2007, 2014; Wang et al., 2013; Xu et al., 2015). Also our estimate of annual  $\text{CH}_4$  budget at the site ( $-0.71\pm 0.06 \text{ g CH}_4 \text{ m}^{-2} \text{ yr}^{-1}$ ) fell within the range of  $-1.6$  to  $-0.18 \text{ CH}_4 \text{ m}^{-2} \text{ yr}^{-1}$  observed in other forest studies (Borken et al., 2006; Luo et al., 2013; Ueyama et al., 2015; Yu et al., 2017), offsetting a mere 0.8 % of the  $\text{CO}_2$  emissions. Winter fluxes contributed a large fraction to the overall  $\text{CH}_4$  budget (14.4–18.4 %), but played a less important role for the  $\text{CO}_2$  budget (6.0–7.3 %), similar to the  $\text{CO}_2$  contribution in other mid latitude and temperate ecosystems (5.5–8.9 %; Gao et al., 2018; Wang et al., 2013) but smaller than some high latitude and other subalpine ecosystems (12–20 %; Kim et al., 2017; Schindlbacher et al., 2007; Xu et al., 2015).

To date, only a few studies have examined soil or forest-floor GHG fluxes in subalpine, temperate, or boreal forests measuring  $\text{CO}_2$ ,  $\text{CH}_4$  and  $\text{N}_2\text{O}$  fluxes in parallel (Tab. 4). Moreover, it is noteworthy that the integration of year-round and temporally highly resolved measurements remains rather uncommon; to our knowledge, only two other studies with year-round measurements exist apart from the current study (Luo et al., 2011; Pilegaard et al., 2003). On the one hand, previous studies frequently measured fluxes for only a limited period of the year, often excluding the dormant season. On the other hand, many of the studies adopted a weekly to monthly measurement frequency, consequently being unable to detect any short-term hot moments, and thus potentially underestimating the flux magnitude. If year-round measurements of forest-floor  $\text{CO}_2$  fluxes are not feasible, using  $Q_{10}$  models might be a viable option, if the annual temperature range is being well covered, as seen in the agreement between our gap-filled continuous measurements and the  $Q_{10}$  budget. However, although  $T_{\text{soil}}$  was identified as the primary driver of  $\text{CO}_2$  emissions, it was not the only one. Thus, neglecting other potential drivers might reduce the reliability and increase the uncertainty of any (modeled) annual  $\text{CO}_2$  budget. Moreover, identifying important drivers for GHG fluxes is the more reliable, the longer and thus typically the more frequent measurements were done. Additionally, to effectively capture the dynamic nature of soil GHG fluxes, it is essential to use of automatic chambers with high temporal resolution, preferentially opaque to exclusively quantify respiration. Therefore, we recommend continuous, year-round measurements to reliably estimate annual forest-floor GHG budgets, particularly when large seasonal variability of potential drivers is expected, or when the duration of the active period, i.e., start and end of the snow-free period, is highly variable like in high elevation or high latitude ecosystems. Particularly with the anticipated impacts of future climate change (IPCC, 2021), duration of growing periods will change, and winter fluxes (or the lack thereof) will gain increasing importance (Xie et al., 2017).

**Tab. 4: Previously published studies investigating forest-floor or soil  $\text{CO}_2$ ,  $\text{CH}_4$  and  $\text{N}_2\text{O}$  fluxes in parallel in temperate, subalpine, or boreal forests using automatic or static chambers.**





Chamber method	Location	Forest type	Years	Duration	# Chambers	Frequency	Reference
Automatic	46.82° N 9.86° E	Subalpine (spruce)	2017, 2020–2022	Year-round	4	3 h	This study
Automatic	39.09° N 75.44° W	Temperate (mixed)	2017	Apr–Jul	3	1 h	Barba et al., 2019
Static	43.23° N 3.20° W	Radiata pine, Douglas fir, beech	2010–2011	Year-round	6	Biweekly	Barrena et al., 2013
Static	37.07° N 119.19° W	Montane mixed-conifer (Mediterranean-type climate)	2010–2012	Year-round	24	Weekly–monthly	Blankinship et al., 2018
Static	35.66° S 148.15° E	Temperate (eucalypt)	2006	2 weeks in Nov	10	4 h	Fest et al., 2009
Static	43.93° N 71.75° W	Northern hardwood (beech, maple, birch)	1998–2000	Year-round	8	Weekly–monthly	Groffman et al., 2006
Static	42.40° N 128.10° E	Broad-leaved Korean pine mixed	2019	Mar–Oct	8	Twice a week–twice a month	Guo et al., 2020
Static	48.09° N 16.01° E	Temperate (beech)	1997	Apr–Nov	8	Biweekly	Hahn et al., 2000
Static	43.83° N 74.87° W	Temperate (mixed)	2008	May–Jul	15	Biweekly	Hopfensperger et al., 2009
Static	47.03° N 8.72° E	subalpine (spruce)	2007–2012	Year-round	10	Every 3 weeks	Krause et al., 2013
Automatic (CO <sub>2</sub> ), static (CH <sub>4</sub> , N <sub>2</sub> O)	48.50° N 11.17° E	Temperate (spruce)	1994–1997, 2000–2010	Year-round	5	1 h (CO <sub>2</sub> ), 2 h (CH <sub>4</sub> , N <sub>2</sub> O)	Luo et al., 2011
Static	46.67– 47.93° N 91.75– 92.52° W	Boreal-temperate (mixed)	2013	May–Oct	48	Monthly	Martins et al., 2017
Static	33.30– 33.47° N 108.35– 108.65° E	Temperate–cold temperate (deciduous broad-leaved & coniferous)	2012–2014	Year-round	60	Weekly–monthly	Pang et al., 2023
Automatic (CO <sub>2</sub> ), static (CH <sub>4</sub> , N <sub>2</sub> O)	55.48° N 11.63° E	Temperate (beech)	1998–1999, 2001	Year-round	5 (CO <sub>2</sub> ), 6 (CH <sub>4</sub> , N <sub>2</sub> O)	2 h (CO <sub>2</sub> ), biweekly (CH <sub>4</sub> , N <sub>2</sub> O)	Pilegaard et al., 2003



Automatic	45.20° N 68.74° W	Sub-boreal (spruce, hemlock)	2013–2016	May– Nov	3-5	30 min	Richardson et al., 2019
Concentration profiles	41.33° N 106.33° W	Subalpine (spruce, fir)	1991–1992	Mar– May	2	Daily– biweekly	Sommerfeld, 1993
Static	49.26– 52.20° N 74.03– 76.07° W	Boreal (black spruce, jack pine, aspen, alder)	2007	May– Oct	48	Monthly	Ullah et al., 2009
Static	57.13° N 14.75° E	Cold temperate (coniferous)	1999–2002	Year-round	30	Weekly– biweekly	Von Arnold et al., 2005
Static	53.28– 53.50° N 122.10– 122.45° E	Cold temperate continental monsoon	2016–2018	Year-round	9	Weekly– monthly	Wu et al., 2019

## 5 Conclusions

We measured year-round GHG fluxes during multiple years with four large opaque automatic chambers and were able to identify their most important drivers. In the light of climate change-induced variations in the onset of the active growing season, growing season length, and winter conditions, we recommend to spatially expand the deployment of such chambers at research stations capable of year-round measurements, including the periods with snow cover. As temperatures will continue to rise due to climate change, and warm and dry conditions, such as in the previous summers, are projected to become more frequent and more severe, we expect an increase in forest-floor GHG emissions at the Davos and similar subalpine or high latitude sites. Anticipated milder winters with reduced snowfall, resulting in shorter snow cover duration and lower average snow depth, will likely contribute to enhanced forest-floor CO<sub>2</sub> emissions and increased forest-floor CH<sub>4</sub> uptake in the future. Since CO<sub>2</sub> emissions are typically much larger than the CH<sub>4</sub> uptake, such as at our site, we expect the forest floor to become a more substantial GHG source in the future, potentially reducing the overall C sink of this type of forest.

*Data availability.* The data used in this study will be made publicly available from the ETH Research Collection (<https://doi.org/10.3929/ethz-b-000619728>, preliminary link).

*Author contributions.* NB designed the study; PM, LK and SB conducted the field work; SB and LK processed the data; LK performed the data analyses, developed the models, and wrote the manuscript draft; SB, MG, PM, IF and NB commented on the manuscript and contributed substantially to discussions and revisions.

*Competing interests.* The authors declare that they have no conflict of interest.

*Acknowledgements.* The authors thank our colleagues Lutz Merbold, Lukas Hörtnagl, Thomas Baur, Werner Eugster and Liliana Scapucci for their assistance in designing and setting up the chambers, conducting fieldwork, and providing helpful

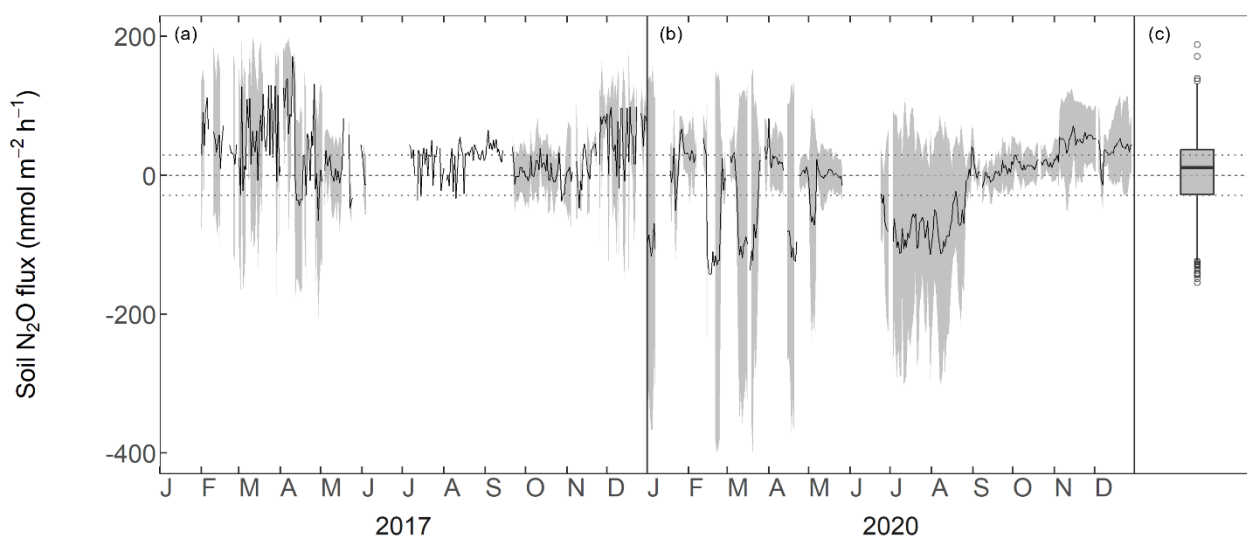


inputs during the flux processing and data interpretation. Their contributions have greatly contributed to the progress of this study.

*Financial support.* This research has been supported by the Swiss National Science Foundation (SNSF), in the projects ICOS-CH Phase 1, 2, 3 (Grant-N° 20FI21\_148992, 20FI20\_173691, 20FI20\_198227) and COCO (Grant-N° 200021\_197357).

410

## A Appendix



415

**Fig. A.1:** Forest-floor  $\text{N}_2\text{O}$  fluxes ( $\text{nmol m}^{-2} \text{h}^{-1}$ ) for the years 2017 (a) and 2020 (b). Black lines show means over four chambers, grey bands show standard deviations among four chambers. Boxplot showing distribution of means over four chambers (c). The dotted lines depict the minimum flux which could be detected by the Dual Quantum Cascade Laser spectrometer.

420

**Tab. A.1:** Details of random forest models used for driver analysis and gap-filling for different time periods (entire year, separately for seasons). Number of observations used to train the models (training set), the hyperparameters “mtry” and “ntree” as well as the  $R^2$  values for observed vs. predicted test data are given. “mtry” specifies how many variables were randomly sampled as candidates at each split, “ntree” indicates the number of trees.

Gas	Time period	No. observations in training set	mtry	ntree	test $R^2$
$\text{CO}_2$	entire year	3111	10	2000	0.95
	spring	860	18	2000	0.94
	summer	623	14	2000	0.73
	autumn	836	14	2000	0.90



CH <sub>4</sub>	winter	774	14	2000	0.63
	entire year	2799	14	2000	0.87
	spring	825	18	2000	0.80
	summer	520	18	2000	0.76
	autumn	772	10	2000	0.72
	winter	674	10	2000	0.73

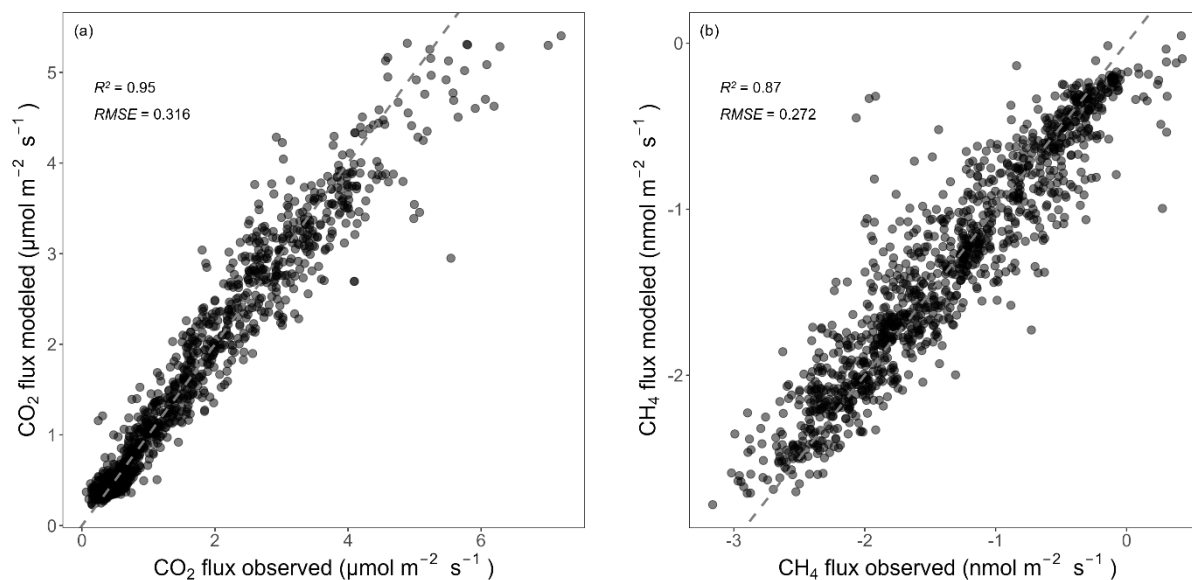


**Fig. A.2: Relationships between observed and predicted (a) CO<sub>2</sub> and (b) CH<sub>4</sub> fluxes from the RF models used for gap filling (only showing test data). R<sup>2</sup> and RSME are given. Black dashed lines mark the 1:1 lines.**

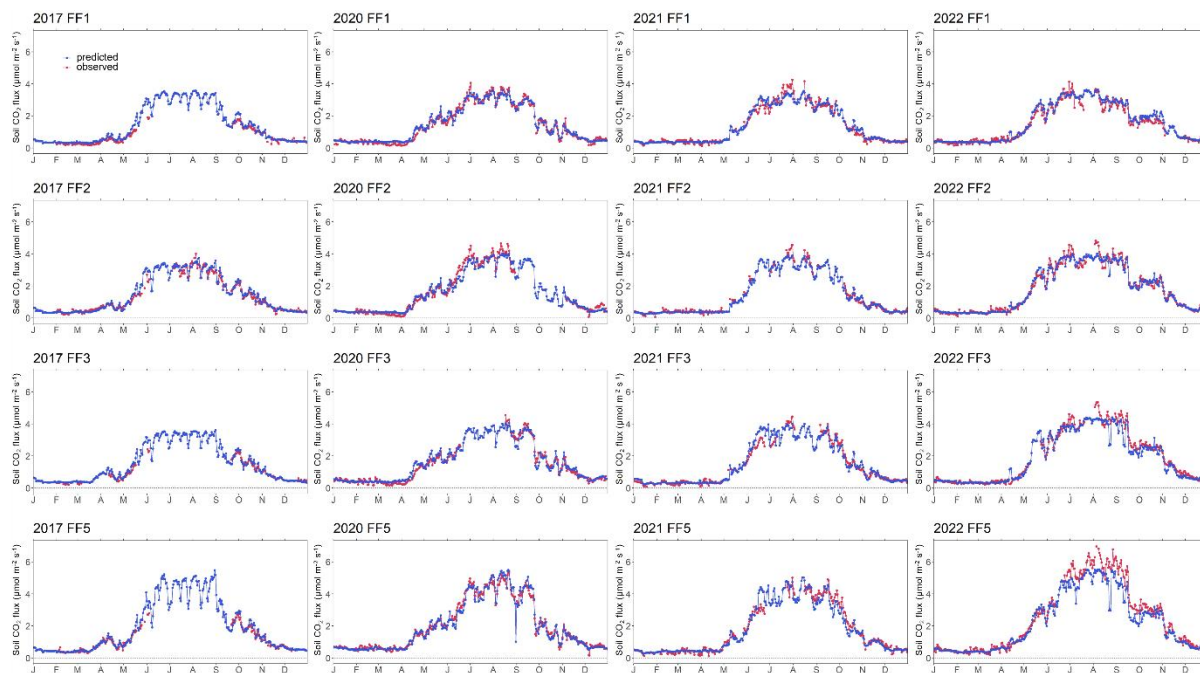


**Fig. A.3: Time series of observed and predicted (using random forest model) forest-floor CO<sub>2</sub> fluxes for four years (2017, 2020–2022) and four chambers (FF1 to FF4).**

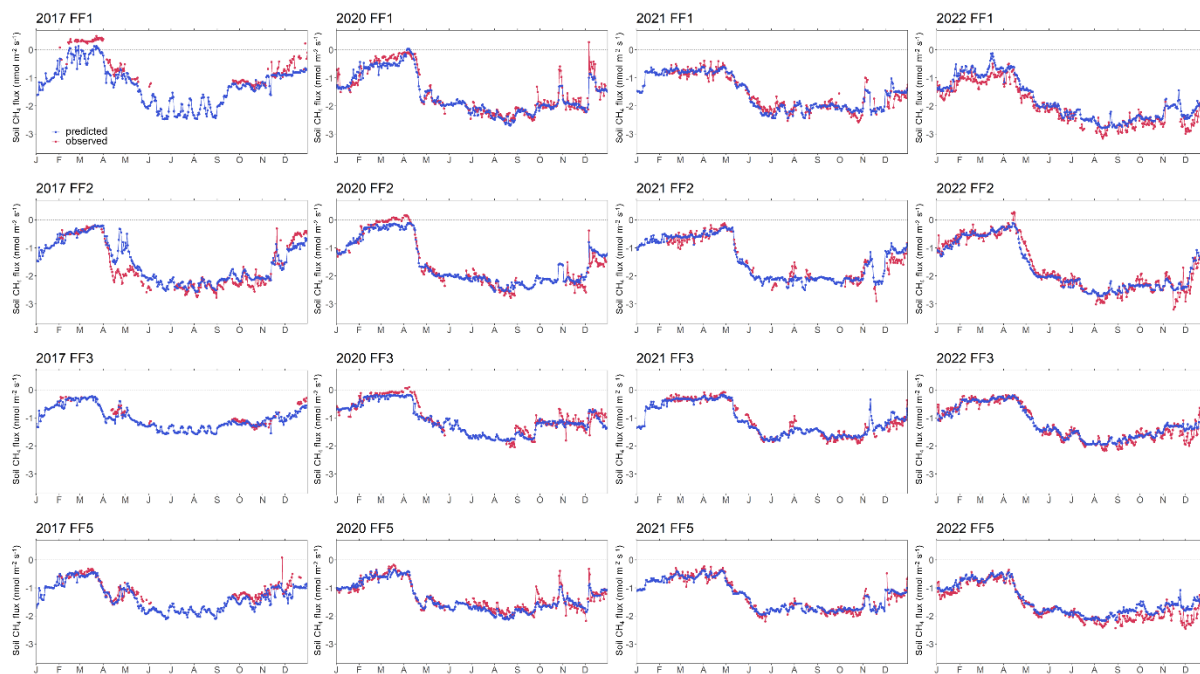
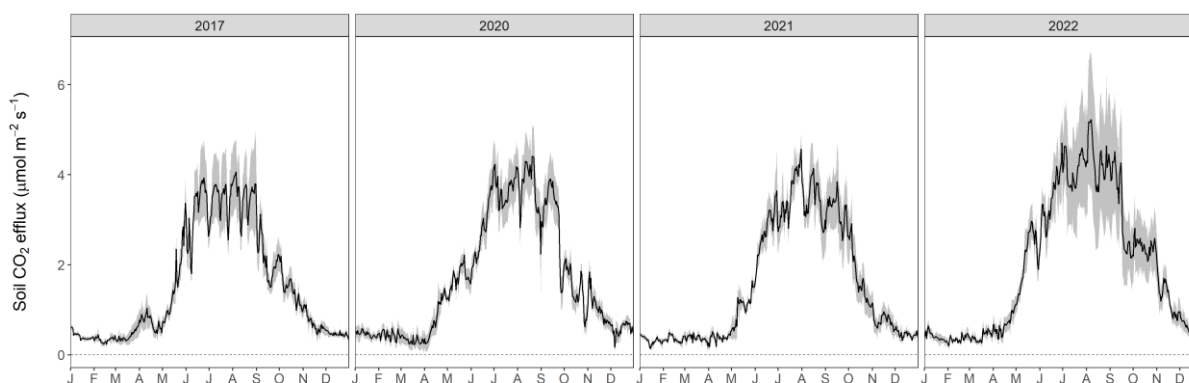




**Fig. A.4: Time series of observed and predicted (using random forest model) forest-floor CH<sub>4</sub> fluxes for four years (2017, 2020–2022) and four chambers (FF1 to FF4).**



435 **Fig. A.5: Gap-filled CO<sub>2</sub> fluxes over four years (grey area: min-max among four chambers).**

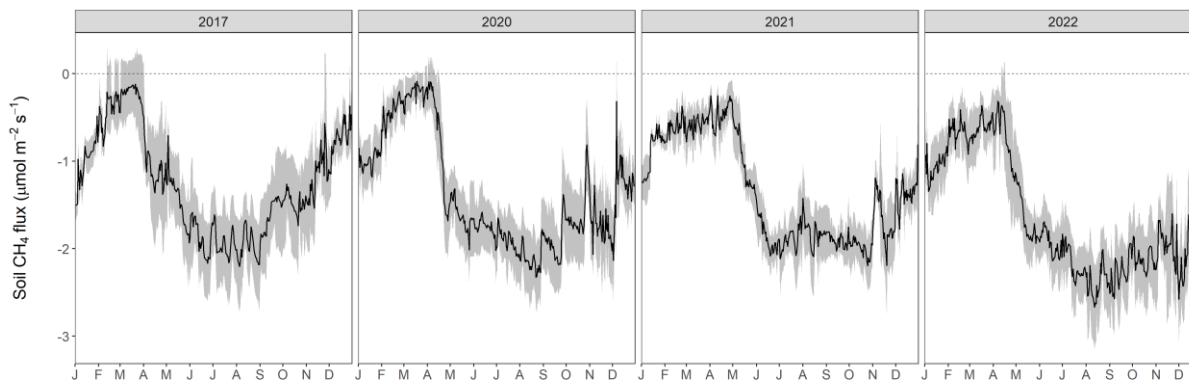


**Fig. A.6: Gap-filled CH<sub>4</sub> fluxes over four years (grey area: min-max among four chambers).**

#### 440 **References**

- Anjileli, H., Huning, L. S., Moftakhari, H., Ashraf, S., Asanjan, A. A., Norouzi, H., and AghaKouchak, A.: Extreme heat events heighten soil respiration, *Sci. Rep.*, 11, 6632, <https://doi.org/10.1038/s41598-021-85764-8>, 2021.
- Arrouays, D., Saby, N. P. A., Boukir, H., Jolivet, C., Ratié, C., Schrumpf, M., Merbold, L., Gielen, B., Gogo, S., Delpierre, N., Vincent, G., Klumpp, K., and Loustau, D.: Soil sampling and preparation for monitoring soil carbon, *Int. Agrophysics*, 32, 633–643, <https://doi.org/10.1515/intag-2017-0047>, 2018.
- 445 Barba, J., Poyatos, R., and Vargas, R.: Automated measurements of greenhouse gases fluxes from tree stems and soils: magnitudes, patterns and drivers, *Sci. Rep.*, 9, 4005, <https://doi.org/10.1038/s41598-019-39663-8>, 2019.



- 450 Barrena, I., Menéndez, S., Duñabeitia, M., Merino, P., Florian Stange, C., Spott, O., González-Murua, C., and Estavillo, J. M.: Greenhouse gas fluxes (CO<sub>2</sub>, N<sub>2</sub>O and CH<sub>4</sub>) from forest soils in the Basque Country: Comparison of different tree species and growth stages, *For. Ecol. Manag.*, 310, 600–611, <https://doi.org/10.1016/j.foreco.2013.08.065>, 2013.
- Basiliko, N., Knowles, R., and Moore, T. R.: Roles of moss species and habitat in methane consumption potential in a northern peatland, 24, 178–185, [https://doi.org/10.1672/0277-5212\(2004\)024\[0178:ROMSAH\]2.0.CO;2](https://doi.org/10.1672/0277-5212(2004)024[0178:ROMSAH]2.0.CO;2), 2004.
- 455 Blankinship, J. C., McCorkle, E. P., Meadows, M. W., and Hart, S. C.: Quantifying the legacy of snowmelt timing on soil greenhouse gas emissions in a seasonally dry montane forest, *Glob. Change Biol.*, 24, 5933–5947, <https://doi.org/10.1111/gcb.14471>, 2018.
- Bond-Lamberty, B., Bailey, V. L., Chen, M., Gough, C. M., and Vargas, R.: Globally rising soil heterotrophic respiration over recent decades, *Nature*, 560, 80–83, <https://doi.org/10.1038/s41586-018-0358-x>, 2018.
- 460 Borken, W., Davidson, E. A., Savage, K., Sundquist, E. T., and Steudler, P.: Effect of summer throughfall exclusion, summer drought, and winter snow cover on methane fluxes in a temperate forest soil, *Soil Biol. Biochem.*, 38, 1388–1395, <https://doi.org/10.1016/j.soilbio.2005.10.011>, 2006.
- Bradford, M. A., Davies, C. A., Frey, S. D., Maddox, T. R., Melillo, J. M., Mohan, J. E., Reynolds, J. F., Treseder, K. K., and Wallenstein, M. D.: Thermal adaptation of soil microbial respiration to elevated temperature, *Ecol. Lett.*, 11, 1316–1327, <https://doi.org/10.1111/j.1461-0248.2008.01251.x>, 2008.
- 465 Brümmer, C., Lyshede, B., Lempio, D., Delorme, J.-P., Ruffer, J. J., Fuß, R., Moffat, A. M., Hurkuck, M., Ibrom, A., Ambus, P., Flessa, H., and Kutsch, W. L.: Gas chromatography vs. quantum cascade laser-based N<sub>2</sub>O flux measurements using a novel chamber design, *Biogeosciences*, 14, 1365–1381, <https://doi.org/10.5194/bg-14-1365-2017>, 2017.
- Carey, J. C., Tang, J., Templer, P. H., Kroeger, K. D., Crowther, T. W., Burton, A. J., Dukes, J. S., Emmett, B., Frey, S. D., Heskell, M. A., Jiang, L., Machmuller, M. B., Mohan, J., Panetta, A. M., Reich, P. B., Reinsch, S., Wang, X., Allison, S. D., Bamminger, C., Bridgham, S., Collins, S. L., de Dato, G., Eddy, W. C., Enquist, B. J., Estiarte, M., Harte, J., Henderson, A., 470 Johnson, B. R., Larsen, K. S., Luo, Y., Marhan, S., Melillo, J. M., Peñuelas, J., Pfeifer-Meister, L., Poll, C., Rastetter, E., Reinmann, A. B., Reynolds, L. L., Schmidt, I. K., Shaver, G. R., Strong, A. L., Suseela, V., and Tietema, A.: Temperature response of soil respiration largely unaltered with experimental warming, *Proc. Natl. Acad. Sci.*, 113, 13797–13802, <https://doi.org/10.1073/pnas.1605365113>, 2016.
- CH2018: CH2018 – Climate Scenarios for Switzerland, Technical Report, National Centre for Climate Services, Zurich, 2018.
- 475 Chapuis-Lardy, L., Wrage, N., Metay, A., Chotte, J.-L., and Bernoux, M.: Soils, a sink for N<sub>2</sub>O? A review, *Glob. Change Biol.*, 13, 1–17, <https://doi.org/10.1111/j.1365-2486.2006.01280.x>, 2007.
- 480 Crowther, T. W., Todd-Brown, K. E. O., Rowe, C. W., Wieder, W. R., Carey, J. C., Machmuller, M. B., Snoek, B. L., Fang, S., Zhou, G., Allison, S. D., Blair, J. M., Bridgham, S. D., Burton, A. J., Carrillo, Y., Reich, P. B., Clark, J. S., Classen, A. T., Dijkstra, F. A., Elberling, B., Emmett, B. A., Estiarte, M., Frey, S. D., Guo, J., Harte, J., Jiang, L., Johnson, B. R., Kröel-Dulay, G., Larsen, K. S., Laudon, H., Lavalley, J. M., Luo, Y., Lupascu, M., Ma, L. N., Marhan, S., Michelsen, A., Mohan, J., Niu, S., Pendall, E., Peñuelas, J., Pfeifer-Meister, L., Poll, C., Reinsch, S., Reynolds, L. L., Schmidt, I. K., Sistla, S., Sokol, N. W., Templer, P. H., Treseder, K. K., Welker, J. M., and Bradford, M. A.: Quantifying global soil carbon losses in response to warming, *Nature*, 540, 104–108, <https://doi.org/10.1038/nature20150>, 2016.
- 485 Danielson, R. E. and Sutherland, P. L.: Porosity, in: *SSSA Book Series*, edited by: Klute, A., Soil Science Society of America, American Society of Agronomy, Madison, WI, USA, 443–461, <https://doi.org/10.2136/sssabookser5.1.2ed.c18>, 2018.



- Debeer, D. and Strobl, C.: Conditional permutation importance revisited, *BMC Bioinformatics*, 21, 307, <https://doi.org/10.1186/s12859-020-03622-2>, 2020.
- Debeer, D., Hothorn, T., and Strobl, C.: permimp: Conditional Permutation Importance, 2021.
- 490 Dutaur, L. and Verchot, L. V.: A global inventory of the soil CH<sub>4</sub> sink, *Glob. Biogeochem. Cycles*, 21, GB4013, <https://doi.org/10.1029/2006GB002734>, 2007.
- Eliasson, P. E., McMurtrie, R. E., Pepper, D. A., Stromgren, M., Linder, S., and Agren, G. I.: The response of heterotrophic CO<sub>2</sub> flux to soil warming, *Glob. Change Biol.*, 11, 167–181, <https://doi.org/10.1111/j.1365-2486.2004.00878.x>, 2005.
- 495 Fest, B. J., Livesley, S. J., Drösler, M., van Gorsel, E., and Arndt, S. K.: Soil–atmosphere greenhouse gas exchange in a cool, temperate *Eucalyptus delegatensis* forest in south-eastern Australia, *Agric. For. Meteorol.*, 149, 393–406, <https://doi.org/10.1016/j.agrformet.2008.09.007>, 2009.
- Fuentes, S., Palmer, A. R., Taylor, D., Zeppel, M., Whitley, R., and Eamus, D.: An automated procedure for estimating the leaf area index (LAI) of woodland ecosystems using digital imagery, MATLAB programming and its application to an examination of the relationship between remotely sensed and field measurements of LAI, *Funct. Plant Biol.*, 35, 1070, <https://doi.org/10.1071/FP08045>, 2008.
- 500 Gao, D., Hagedorn, F., Zhang, L., Liu, J., Qu, G., Sun, J., Peng, B., Fan, Z., Zheng, J., Jiang, P., and Bai, E.: Small and transient response of winter soil respiration and microbial communities to altered snow depth in a mid-temperate forest, *Appl. Soil Ecol.*, 130, 40–49, <https://doi.org/10.1016/j.apsoil.2018.05.010>, 2018.
- Gaumont-Guay, D., Black, T. A., Barr, A. G., Griffis, T. J., Jassal, R. S., Krishnan, P., Grant, N., and Nesic, Z.: Eight years of forest-floor CO<sub>2</sub> exchange in a boreal black spruce forest: Spatial integration and long-term temporal trends, *Agric. For. Meteorol.*, 184, 25–35, <https://doi.org/10.1016/j.agrformet.2013.08.010>, 2014.
- 505 Goldberg, S. D., Borken, W., and Gebauer, G.: N<sub>2</sub>O emission in a Norway spruce forest due to soil frost: concentration and isotope profiles shed a new light on an old story, *Biogeochemistry*, 97, 21–30, <https://doi.org/10.1007/s10533-009-9294-z>, 2010.
- Goldman, M. B., Groffman, P. M., Pouyat, R. V., McDonnell, M. J., and Pickett, S. T. A.: CH<sub>4</sub> uptake and N availability in forest soils along an urban to rural gradient, *Soil Biol. Biochem.*, 27, 281–286, [https://doi.org/10.1016/0038-0717\(94\)00185-4](https://doi.org/10.1016/0038-0717(94)00185-4), 1995.
- 510 Goldstein, A., Kapelner, A., Bleich, J., and Pitkin, E.: Peeking inside the black box: Visualizing statistical learning with plots of individual conditional expectation, *J. Comput. Graph. Stat.*, 24, 44–65, <https://doi.org/10.1080/10618600.2014.907095>, 2015.
- 515 Greenwell, B., M.: pdp: An R package for constructing partial dependence plots, *R J.*, 9, 421, <https://doi.org/10.32614/RJ-2017-016>, 2017.
- Groffman, P. M., Hardy, J. P., Driscoll, C. T., and Fahey, T. J.: Snow depth, soil freezing, and fluxes of carbon dioxide, nitrous oxide and methane in a northern hardwood forest, *Glob. Change Biol.*, 12, 1748–1760, <https://doi.org/10.1111/j.1365-2486.2006.01194.x>, 2006.
- 520 Guo, C., Zhang, L., Li, S., Li, Q., and Dai, G.: Comparison of Soil Greenhouse Gas Fluxes during the Spring Freeze–Thaw Period and the Growing Season in a Temperate Broadleaved Korean Pine Forest, Changbai Mountains, China, *Forests*, 11, 1135, <https://doi.org/10.3390/f11111135>, 2020.





- Hahn, M., Gartner, K., and Zechmeister-Boltenstern, S.: Greenhouse gas emissions (N<sub>2</sub>O, CO<sub>2</sub> and CH<sub>4</sub>) from three forest soils near Vienna (Austria) with different water and nitrogen regimes, *Bodenkultur*, 51, 115–125, 2000.
- 525 Hanson, P. J., Edwards, N. T., Garten, C. T., and Andrews, J. A.: Separating root and soil microbial contributions to soil respiration: A review of methods and observations, *Biogeochemistry*, 48, 115–146, <https://doi.org/10.1023/A:1006244819642>, 2000.
- Hartley, I. P., Heinemeyer, A., and Ineson, P.: Effects of three years of soil warming and shading on the rate of soil respiration: substrate availability and not thermal acclimation mediates observed response, *Glob. Change Biol.*, 13, 1761–1770, 530 <https://doi.org/10.1111/j.1365-2486.2007.01373.x>, 2007.
- Högberg, P., Nordgren, A., Buchmann, N., Taylor, A. F. S., Ekblad, A., Högberg, M. N., Nyberg, G., Ottosson-Löfvenius, M., and Read, D. J.: Large-scale forest girdling shows that current photosynthesis drives soil respiration, *Nature*, 411, 789–792, <https://doi.org/10.1038/35081058>, 2001.
- Hopfensperger, K. N., Gault, C. M., and Groffman, P. M.: Influence of plant communities and soil properties on trace gas 535 fluxes in riparian northern hardwood forests, *For. Ecol. Manag.*, 258, 2076–2082, <https://doi.org/10.1016/j.foreco.2009.08.004>, 2009.
- IPCC: Climate change 2021: The physical science basis. Contribution of working group I to the sixth assessment report of the Intergovernmental Panel on Climate Change, Cambridge University Press, Chambride, United Kingdom and New York, NY, USA, 2021.
- 540 Janssens, I. A., Lankreijer, H., Matteucci, G., Kowalski, A. S., Buchmann, N., Epron, D., Pilegaard, K., Kutsch, W., Longdoz, B., Grünwald, T., Montagnani, L., Dore, S., Rebmann, C., Moors, E. J., Grelle, A., Rannik, Ü., Morgenstern, K., Oltchev, S., Clement, R., Guðmundsson, J., Minerbi, S., Berbigier, P., Ibrom, A., Moncrieff, J., Aubinet, M., Bernhofer, C., Jensen, N. O., Vesala, T., Granier, A., Schulze, E.-D., Lindroth, A., Dolman, A. J., Jarvis, P. G., Ceulemans, R., and Valentini, R.: Productivity overshadows temperature in determining soil and ecosystem respiration across European forests, *Glob. Change* 545 *Biol.*, 7, 269–278, <https://doi.org/10.1046/j.1365-2486.2001.00412.x>, 2001.
- Jörg, S.: Böden im Seehornwald bei Davos und deren Vorrat an Kohlenstoff und Stickstoff. Diplomarbeit, Zürcher Hochschule für Angewandte Wissenschaften, Zürcher Hochschule für Angewandte Wissenschaften, Zurich, 79 pp., 2008.
- Karhu, K., Auffret, M. D., Dungait, J. A. J., Hopkins, D. W., Prosser, J. I., Singh, B. K., Subke, J.-A., Wookey, P. A., Ågren, G. I., Sebastià, M.-T., Gouriveau, F., Bergkvist, G., Meir, P., Nottingham, A. T., Salinas, N., and Hartley, I. P.: Temperature 550 sensitivity of soil respiration rates enhanced by microbial community response, *Nature*, 513, 81–84, <https://doi.org/10.1038/nature13604>, 2014.
- Kim, Y., Kodama, Y., and Fochesatto, G. J.: Environmental factors regulating winter CO<sub>2</sub> flux in snow-covered black forest soil of Interior Alaska, *Geochem. J.*, 51, 359–371, <https://doi.org/10.2343/geochemj.2.0475>, 2017.
- Klein, G., Vitasse, Y., Rixen, C., Marty, C., and Rebetez, M.: Shorter snow cover duration since 1970 in the Swiss Alps due 555 to earlier snowmelt more than to later snow onset, *Clim. Change*, 139, 637–649, <https://doi.org/10.1007/s10584-016-1806-y>, 2016.
- Krause, K., Niklaus, P. A., and Schleppei, P.: Soil-atmosphere fluxes of the greenhouse gases CO<sub>2</sub>, CH<sub>4</sub> and N<sub>2</sub>O in a mountain spruce forest subjected to long-term N addition and to tree girdling, *Agric. For. Meteorol.*, 181, 61–68, <https://doi.org/10.1016/j.agrformet.2013.07.007>, 2013.



- 560 Kuhn, M.: Building Predictive Models in R Using the caret Package, *J. Stat. Softw.*, 28, 1–26, <https://doi.org/10.18637/jss.v028.i05>, 2008.
- Liu, S., Schloter, M., and Brüggemann, N.: Accumulation of  $\text{NO}_2^-$  during periods of drying stimulates soil  $\text{N}_2\text{O}$  emissions during subsequent rewetting: Nitrite stimulates  $\text{N}_2\text{O}$  emissions during rewetting, *Eur. J. Soil Sci.*, 69, 936–946, <https://doi.org/10.1111/ejss.12683>, 2018.
- 565 Luedeling, E. and Fernandez, E.: chillR: Statistical methods for phenology analysis in temperate fruit, 2022.
- Luo, G., Brüggemann, N., Wolf, B., Gasche, R., Grote, R., and Butterbach-Bahl, K.: Decadal variability of soil  $\text{CO}_2$ ,  $\text{NO}$ ,  $\text{N}_2\text{O}$ , and  $\text{CH}_4$  fluxes at the Höglwald Forest, Germany, *Biogeosciences*, 9, 1741–1763, <https://doi.org/10.5194/BG-9-1741-2012>, 2011.
- Luo, G. J., Kiese, R., Wolf, B., and Butterbach-Bahl, K.: Effects of soil temperature and moisture on methane uptake and nitrous oxide emissions across three different ecosystem types, *Biogeosciences*, 10, 3205–3219, <https://doi.org/10.5194/bg-10-3205-2013>, 2013.
- Martins, C. S. C., Nazaries, L., Delgado-Baquerizo, M., Macdonald, C. A., Anderson, I. C., Hobbie, S. E., Venterea, R. T., Reich, P. B., and Singh, B. K.: Identifying environmental drivers of greenhouse gas emissions under warming and reduced rainfall in boreal–temperate forests, *Funct. Ecol.*, 31, 2356–2368, <https://doi.org/10.1111/1365-2435.12928>, 2017.
- 575 Martinson, G. O., Müller, A. K., Matson, A. L., Corre, M. D., and Veldkamp, E.: Nitrogen and Phosphorus Control Soil Methane Uptake in Tropical Montane Forests, *J. Geophys. Res. Biogeosciences*, 126(8), e2020JG005970, <https://doi.org/10.1029/2020JG005970>, 2021.
- McManus, J. B., Nelson, D. D., Herndon, S. C., Shorter, J. H., Zahniser, M. S., Blaser, S., Hvozدارa, L., Muller, A., Giovannini, M., and Faist, J.: Comparison of cw and pulsed operation with a TE-cooled quantum cascade infrared laser for detection of nitric oxide at 1900  $\text{cm}^{-1}$ , *Appl. Phys. B*, 85, 235–241, <https://doi.org/10.1007/s00340-006-2407-7>, 2006.
- 580 Melillo, J. M., Frey, S. D., DeAngelis, K. M., Werner, W. J., Bernard, M. J., Bowles, F. P., Pold, G., Knorr, M. A., and Grandy, A. S.: Long-term pattern and magnitude of soil carbon feedback to the climate system in a warming world, *Science*, 358, 101–105, <https://doi.org/10.1126/science.aan2874>, 2017.
- Ni, X. and Groffman, P. M.: Declines in methane uptake in forest soils, *Proc. Natl. Acad. Sci.*, 115, 8587–8590, <https://doi.org/10.1073/pnas.1807377115>, 2018.
- 585 Pang, J., Peng, C., Wang, X., Zhang, H., and Zhang, S.: Soil-atmosphere exchange of carbon dioxide, methane and nitrous oxide in temperate forests along an elevation gradient in the Qinling Mountains, China, *Plant Soil*, <https://doi.org/10.1007/s11104-023-05967-y>, 2023.
- Papen, H. and Butterbach-Bahl, K.: A 3-year continuous record of nitrogen trace gas fluxes from untreated and limed soil of a N-saturated spruce and beech forest ecosystem in Germany: 1.  $\text{N}_2\text{O}$  emissions, *J. Geophys. Res. Atmospheres*, 104, 18487–18503, <https://doi.org/10.1029/1999JD900293>, 1999.
- 590 Pavelka, M., Acosta, M., Kiese, R., Altimir, N., Brümmner, C., Crill, P., Darenova, E., Fuß, R., Gielen, B., Graf, A., Klemetsson, L., Lohila, A., Longdoz, B., Lindroth, A., Nilsson, M., Jiménez, S. M., Merbold, L., Montagnani, L., Peichl, M., Pihlatie, M., Pumpanen, J., Ortiz, P. S., Silvennoinen, H., Skiba, U., Vestin, P., Weslien, P., Janous, D., and Kutsch, W.: Standardisation of chamber technique for  $\text{CO}_2$ ,  $\text{N}_2\text{O}$  and  $\text{CH}_4$  fluxes measurements from terrestrial ecosystems, *Int. Agrophysics*, 32, 569–587, <https://doi.org/10.1515/intag-2017-0045>, 2018.



- Pilegaard, K., Mikkelsen, T. N., Beier, C., Jensen, N. O., Ambus, P., and Ro-Poulsen, H.: Field measurements of atmosphere–biosphere interactions in a Danish beech forest, *Boreal Environ. Res.*, 8, 315–333, 2003.
- 600 R Core Team: R: A language and environment for statistical computing, R Foundation for Statistical Computing, Vienna, Austria, 2022.
- Reinmann, A. B. and Templer, P. H.: Increased soil respiration in response to experimentally reduced snow cover and increased soil freezing in a temperate deciduous forest, *Biogeochemistry*, 140, 359–371, <https://doi.org/10.1007/s10533-018-0497-z>, 2018.
- 605 Richardson, A. D., Hollinger, D. Y., Shoemaker, J. K., Hughes, H., Savage, K., and Davidson, E. A.: Six years of ecosystem-atmosphere greenhouse gas fluxes measured in a sub-boreal forest, *Sci. Data*, 6, 117, <https://doi.org/10.1038/s41597-019-0119-1>, 2019.
- Robette, N.: moreparty: A toolbox for conditional inference trees and random forests, 2023.
- Saunois, M., Stavert, A. R., Poulter, B., Bousquet, P., Canadell, J. G., Jackson, R. B., Raymond, P. A., Dlugokencky, E. J., Houweling, S., Patra, P. K., Ciais, P., Arora, V. K., Bastviken, D., Bergamaschi, P., Blake, D. R., Brailsford, G., Bruhwiler, L., Carlson, K. M., Carrol, M., Castaldi, S., Chandra, N., Crevoisier, C., Crill, P. M., Covey, K., Curry, C. L., Etiope, G., Frankenberg, C., Gedney, N., Hegglin, M. I., Höglund-Isaksson, L., Hugelius, G., Ishizawa, M., Ito, A., Janssens-Maenhout, G., Jensen, K. M., Joos, F., Kleinen, T., Krummel, P. B., Langenfelds, R. L., Laruelle, G. G., Liu, L., Machida, T., Maksyutov, S., McDonald, K. C., McNorton, J., Miller, P. A., Melton, J. R., Morino, I., Müller, J., Murguía-Flores, F., Naik, V., Niwa, Y., Noce, S., O’Doherty, S., Parker, R. J., Peng, C., Peng, S., Peters, G. P., Prigent, C., Prinn, R., Ramonet, M., Regnier, P., Riley, W. J., Rosentreter, J. A., Segers, A., Simpson, I. J., Shi, H., Smith, S. J., Steele, L. P., Thornton, B. F., Tian, H., Tohjima, Y., Tubiello, F. N., Tsuruta, A., Viovy, N., Voulgarakis, A., Weber, T. S., van Weele, M., van der Werf, G. R., Weiss, R. F., Worthy, D., Wunch, D., Yin, Y., Yoshida, Y., Zhang, W., Zhang, Z., Zhao, Y., Zheng, B., Zhu, Q., Zhu, Q., and Zhuang, Q.: The Global Methane Budget 2000–2017, *Earth Syst. Sci. Data*, 12, 1561–1623, <https://doi.org/10.5194/essd-12-1561-2020>, 2020.
- 610 620 Schaufler, G., Kitzler, B., Schindlbacher, A., Skiba, U., Sutton, M., and Zechmeister-Boltenstern, S.: Greenhouse gas emissions from European soils under different land use: effects of soil moisture and temperature, *Eur. J. Soil Sci.*, 61, 683–696, <https://doi.org/10.1111/j.1365-2389.2010.01277.x>, 2010.
- Schindlbacher, A., Zechmeister-Boltenstern, S., Glatzel, G., and Jandl, R.: Winter soil respiration from an Austrian mountain forest, *Agric. For. Meteorol.*, 146, 205–215, <https://doi.org/10.1016/j.agrformet.2007.06.001>, 2007.
- 625 Schindlbacher, A., Jandl, R., and Schindlbacher, S.: Natural variations in snow cover do not affect the annual soil CO<sub>2</sub> from a mid-elevation temperate forest, *Glob. Change Biol.*, 20, 622–632, <https://doi.org/10.1111/gcb.12367>, 2014.
- Scott-Denton, L. E., Rosenstiel, T. N., and Monson, R. K.: Differential controls by climate and substrate over the heterotrophic and rhizospheric components of soil respiration: Controls over soil respiration, *Glob. Change Biol.*, 12, 205–216, <https://doi.org/10.1111/j.1365-2486.2005.01064.x>, 2006.
- 630 Sommerfeld, R. A.: CO<sub>2</sub>, CH<sub>4</sub> and N<sub>2</sub>O flux through a Wyoming snowpack and implications for global budgets, 361, 140–142, 1993.
- Song, Y., Zou, Y., Wang, G., and Yu, X.: Altered soil carbon and nitrogen cycles due to the freeze-thaw effect: A meta-analysis, *Soil Biol. Biochem.*, 109, 35–49, <https://doi.org/10.1016/j.soilbio.2017.01.020>, 2017.



- 635 Strobl, C., Boulesteix, A.-L., Zeileis, A., and Hothorn, T.: Bias in random forest variable importance measures: Illustrations, sources and a solution, *BMC Bioinformatics*, 8, 25, <https://doi.org/10.1186/1471-2105-8-25>, 2007.
- Strobl, C., Boulesteix, A.-L., Kneib, T., Augustin, T., and Zeileis, A.: Conditional variable importance for random forests, *BMC Bioinformatics*, 9, 307, <https://doi.org/10.1186/1471-2105-9-307>, 2008.
- Tschopp, T.: Zur Geschichte des Seehornwaldes in Davos. Praktikumsarbeit, WSL, Birmensdorf, 2012.
- 640 Ueyama, M., Takeuchi, R., Takahashi, Y., Ide, R., Ataka, M., Kosugi, Y., Takahashi, K., and Saigusa, N.: Methane uptake in a temperate forest soil using continuous closed-chamber measurements, *Agric. For. Meteorol.*, 213, 1–9, <https://doi.org/10.1016/j.agrformet.2015.05.004>, 2015.
- Ullah, S., Frasier, R., Pelletier, L., and Moore, T. R.: Greenhouse gas fluxes from boreal forest soils during the snow-free period in Quebec, Canada, *Can. J. For. Res.*, 39, 666–680, <https://doi.org/10.1139/X08-209>, 2009.
- 645 Von Arnold, K., Weslien, P., Nilsson, M., Svensson, B. H., and Klemedtsson, L.: Fluxes of CO<sub>2</sub>, CH<sub>4</sub> and N<sub>2</sub>O from drained coniferous forests on organic soils, *For. Ecol. Manag.*, 210, 239–254, <https://doi.org/10.1016/j.foreco.2005.02.031>, 2005.
- Wang, C., Han, Y., Chen, J., Wang, X., Zhang, Q., and Bond-Lamberty, B.: Seasonality of soil CO<sub>2</sub> efflux in a temperate forest: Biophysical effects of snowpack and spring freeze–thaw cycles, *Agric. For. Meteorol.*, 177, 83–92, <https://doi.org/10.1016/j.agrformet.2013.04.008>, 2013.
- 650 Wu, X., Zang, S., Ma, D., Ren, J., Chen, Q., and Dong, X.: Emissions of CO<sub>2</sub>, CH<sub>4</sub>, and N<sub>2</sub>O Fluxes from Forest Soil in Permafrost Region of Daxing’an Mountains, Northeast China, *Int. J. Environ. Res. Public Health*, 16, 2999, <https://doi.org/10.3390/ijerph16162999>, 2019.
- Xie, J., Kneubühler, M., Garonna, I., Notarnicola, C., De Gregorio, L., De Jong, R., Chimani, B., and Schaepman, M. E.: Altitude-dependent influence of snow cover on alpine land surface phenology: Snow cover and Alpine phenology, *J. Geophys. Res. Biogeosciences*, 122, 1107–1122, <https://doi.org/10.1002/2016JG003728>, 2017.
- 655 Xu, Z., Zhou, F., Yin, H., and Liu, Q.: Winter soil CO<sub>2</sub> efflux in two contrasting forest ecosystems on the eastern Tibetan Plateau, China, *J. For. Res.*, 26, 679–686, <https://doi.org/10.1007/s11676-015-0120-2>, 2015.
- Yu, L., Huang, Y., Zhang, W., Li, T., and Sun, W.: Methane uptake in global forest and grassland soils from 1981 to 2010, *Sci. Total Environ.*, 607–608, 1163–1172, <https://doi.org/10.1016/j.scitotenv.2017.07.082>, 2017.
- 660 Yuste, J. C., Nagy, M., Janssens, I. A., Carrara, A., and Ceulemans, R.: Soil respiration in a mixed temperate forest and its contribution to total ecosystem respiration, *Tree Physiol.*, 25, 609–619, <https://doi.org/10.1093/treephys/25.5.609>, 2005.
- Zielis, S., Etzold, S., Zweifel, R., Eugster, W., Haeni, M., and Buchmann, N.: NEP of a Swiss subalpine forest is significantly driven not only by current but also by previous year’s weather, *Biogeosciences*, 11, 1627–1635, <https://doi.org/10.5194/bg-11-1627-2014>, 2014.